Journal of
Engineering Sciences
Faculty of Engineering
Assiut University
JES
مجلة
العلوم الهندسية
كلية الهندسة
جامعة أسيوط
journal homepage: http://jesaun.journals.ekb.eg

Combined Effect of Seismic-Induced Collision and Soil Stress Irregularity on Seismic Response of Adjacent High-Rise Buildings: Evaluation and Mitigation

Received 12 October 2022; Revised 15 November 2022; Accepted 23 November 2022

Manar A. Ahmed*[1]
Ahmed. A. Farghaly[2]

Keywords
adjacent high-rise buildings; irregular soil stresses; seismic pounding mitigation; seismic response; soil-structure interaction

Abstract

Unequal distribution of stresses in soil underneath the foundations of adjacent buildings represents a great challenge in structural engineering, especially for buildings prone to earthquakes. Another serious problem facing earthquake-prone adjacent buildings is collision, which severely affects the behaviour of the buildings and changes the distribution of the soil stresses under the foundations of the buildings. This research investigates seismic responses of adjacent High-Rise Buildings (HRBs) exposed to seismic-induced pounding and impose irregular soil stress distribution considering the Soil-Structure Interaction (SSI) effect. For this purpose, numerical nonlinear dynamic analysis of three-dimensional models of adjacent four HRBs is conducted. To mitigate the exaggerated effect of seismic-induced collision and soil stress irregularity on the seismic response of the adjacent HRBs, three approaches are proposed; improving soil bearing capacity in the highly stressed zone, joining the adjacent HRBs by means of Fluid Viscous Links (FVLs), and combining the two previous approaches. Three-dimensional models of the adjacent 4HRBs group are studied under different earthquakes to examine the above-mentioned three approaches. The combination approach shows promising results in moderating the collision effects; it considerably mitigates the pounding effects between the adjacent HRBs in terms of reducing straining actions and displacements of buildings as well as controlling stresses irregularity in soil under the foundations of such buildings.

1. Introduction

The lack of construction land leads to the adhesion of buildings, and thus, to the inability to extend the prominence of raft foundations, which means cutting dimensions on the boundaries of the adjacent buildings. Consequently, the stresses in the soil beneath the raft foundation become irregular. Contiguous buildings lead to intensified stresses in some regions in the soil beneath the foundation. Besides, collision between the superstructures of the adjacent buildings as well as in the

[1] Assoc. Professor, Dept. of Civil Engineering, Faculty of Engineering, Suez Canal University, Ismailia, Egypt.
manar_abdelshakour@eng.suez.edu.eg,
[2]Prof., Dept. of Civil and Architectural Constructions, Faculty of Technology and Education, Sohag University, Sohag, Egypt.
khodary20002000@yahoo.com

https://doi.org/10.21608/JESAUN.2022.167818.1172
This is an open access article under the CC BY-NC-ND license (http://creativecommons.org/licenses/by-nc-nd/4.0/).

foundations level has high amplitude and short duration effects cause localized degradation of the stiffness and strength in the affected members and leave an overall modification in the behavior of the structures and the stresses distribution in the soil under the foundation of the buildings.

Pounding mitigation between adjacent buildings during earthquakes has been the concern of considerable research. Jankowski and Mahmoud [1] mitigated the pounding effect between two adjacent buildings through three types of links (spring, damper, and spring-damper-like elements). It was concluded that the large stiffness or damping values are more effective in decreasing the pounding effect. On the other hand, they confirmed that the use of visco-elastic elements reduces the peak displacement of the lighter and more flexible building at lower stiffness and damping values compared to the case when spring or damper elements are applied alone. Barros and Khatami [2] checked the pounding force between two adjacent buildings connected with links and suggested new formulas and confirmed that the top of buildings is the most part suffer from pounding. Licari et al. [3] proposed a retrofit technique reproducing Jankowski's nonlinear viscoelastic relationships as a mitigation solution for the pounding of adjacent buildings. Polycarpou and Komodromos [4] used rubber bumpers to mitigate the pounding effect under heavy earthquakes and studied the effect of gap size, earthquake characteristics, and thickness, compressive capacity, and damping of the rubber bumpers. Lin et al. [5] used Pounding Tuned Mass Damper (PTMD) to mitigate the pounding effects of the adjacent buildings experimentally by applying the manufactured PTMD on a shaking table, the results showed that the TMD is sensitive to input excitations, while the PTMD mostly has improved control performance over the TMD. Skrekas et al. [6] studied the inelastic response of two 5-storey buildings with a 7-storey building. It was shown that the effect of the induced torsion on the structural response of the entire block is substantial due to the bi-directional seismic pounding because of the coupled building block system. Khatiwada et al. [7] applied a parametric study of mass pendulums, relative velocities, and shape of contact surface on the restitution and acceleration. It was concluded that acceleration is not dependent on mass but on velocity, total participating mass, and the ratio of striker mass to struck block. Polycarpou et al. [8] applied numerical simulations and parametric studies on the effect of the inclination angle of the earthquake on adjacent buildings as a very important parameter during pounding. Lin et al. [9] used a Multiple Pounding Tuned Mass Damper (MPTMD) to reduce the pounding between two adjacent buildings and obtained an equation that controls the response. The (MPTMD) was applied on an existing tower, it was concluded that the system has better control efficiency over the traditional TMDs. Amiri et al. [10] studied the base isolation effect on the adjacent non-isolated base buildings. The results indicated that the effect of the stiffness of the adjacent buildings on the impact imposed on the superstructure, and the increment of the fundamental period of the isolated building could intensify the impact force up to nearly five-fold. Bi et al. [11] studied the pounding between L-shaped irregular 3D buildings with numerical simulations and investigated the different parameters of the pounding on the response of each building with the probability of the pounding locations. Kheyroddin et al. [12] studied the lateral structural systems of adjacent earthquake-resistant buildings to show which system can mitigate the pounding between these buildings under earthquake. Jiang et al. [13] studied the pounding between unequal height adjacent low-rise buildings with a parametric study on the different parameters that affect the pounding and concluded that the dangerous pounding is at mid-column. Karabork et al. [14] found the optimum placements of viscous dampers to prevent the pounding between adjacent buildings with a new algorithm and improved its effectiveness. Abdel Raheem et al. [15] studied the eccentric pounding

between adjacent buildings and concluded that torsional oscillation due to eccentric pounding plays a significant role in the overall response of symmetric buildings in horizontal eccentric alignment under earthquake excitation. Shi et al. [16] described the effect of contact pounding points of adjacent buildings subjected to earthquakes and concluded that the hierarchical substructure method can significantly speed up the numeric integration procedure by preserving a required level of accuracy. Abdel Raheem et al. [17] studied the pounding effect on the adjacent buildings and the effect of the number of stores, separation distances, and alignment configurations on the behavior of the adjacent buildings. It was concluded that the pounding effects depend on the dynamic characteristics and produce big acceleration and shear force. Naserkhaki et al. [18] studied the pounding between adjacent buildings and concluded that the taller building is not affected when the short building is relatively very short. But it will suffer if the height of the short building is increased, and the most critical pounding scenario is when the shorter building's height is half of the height of the taller one, which demands increasing the separation gap. Rahimi and Soltanim [19] proposed an analytical approach for the pounding of adjacent buildings and showed that the proposed approach can significantly save computational costs by obviating the need for performing dynamic analysis. Shehata E. A. et al. [20] compared the seismic response of structures with shallow raft base lying on soft soil with fixed support conditions. F. Kazemi et al. [21] studied adjacent RC and steel moment-resisting frame buildings with different heights to investigate the collision effects. The results illustrated that providing a fluid viscous damper between adjacent reinforced concrete and steel structures can be effective to eliminate the sudden changes in the lateral forces during the collision. Farghaly [22] studied the effect of soil-structure interaction on the seismic response of adjacent buildings and investigated the effect of pounding between the superstructure and the substructure at the foundation level for buildings with different heights and different foundation levels.

Several studies have contributed significantly to the field of seismic-induced pounding between buildings and the influential factors in the pounding phenomenon. However, the dynamic interaction between buildings undergoing pounding and the surrounding soil is worthy of further consideration. In general, the interaction effect between soil and structure is disregarded during seismic design and analysis of superstructures. However, the system of soil-base adversely affects the behaviour of the structures; the response of a structure supported on a rigid foundation to earthquake motion is not the same response as if the structure is supported on deformable soil. Moreover, recorded ground motion at the base of a structure is different from that which would be recorded if there is no structure. The assumption of ignoring the effects of SSI might be appropriate for rigid soil. For soft soils, the response of the structure under seismic excitation is significantly influenced by SSI [23]. It has been recognized that SSI decreases the stiffness of the structure due to the movement of the flexible soil [24]. Miari et al. [25] extensively reviewed previous studies on pounding between adjacent buildings with fixed bases, isolated buildings, and buildings resting on soft soils. Previous studies concerning the factors that influence earthquake-induced structural pounding in bridge structures were reviewed by Miari et al. [26] and recommended mitigation measures were introduced.

The flexible structure was found to be more sensitive to pounding with SSI compared to the stiffer structure [27–29]. Most studies indicate that the response of the superstructure regarding displacement, shear forces, pounding forces, base forces, and acceleration is higher in the case when SSI is considered. In other studies, it was found that considering SSI leads to a reduction in the peak

displacements, shear forces, impact forces, and energy dissipation, while it leads to an increase in the acceleration at all storeys and the number of impacts. The difference in the results is attributed to the type of soil and the foundation type used in investigations. The influence of the soil type on the effects of collision between buildings is also investigated by M. Miari et al. [30,31]. These studies investigated the effect of pounding between buildings founded on the same and different soil types. Three 3-D high-rise buildings with different heights experiencing earthquake-induced pounding were examined considering five different soil types defined in the ASCE 7-10 code. The results of this study indicate that higher displacements at all storeys, peak storey shears, and pounding forces were experienced in buildings founded on soft clay soil, then for buildings founded on stiff soil, then for buildings founded on very dense soil and soft rock, and finally for buildings founded on rock and hard rock. This means that considering the soil-structure interaction and the soil type in pounding studies is crucial rather than considering fixed-base building. Mahmoud et al. [32] investigated the influence of SSI on isolated buildings with rubber bearings subjected to pounding with moat wall. The results showed that, regarding the superstructure response, the displacement, acceleration, and number of impacts increase while the impact force and dissipated energy decrease when taking SSI into consideration. Regarding the isolated base, the acceleration decreases while the displacement is insensitive considering SSI. The response is greater when the soil is softer and when the ground motion is near the site. The general aim of this paper is to contribute to understanding the response of high-rise adjacent buildings vulnerable to seismic-induced pounding considering SSI effect.

2. Research Objective

The main objectives of this paper are to study the pounding effect between adjacent HRBs imposing unequal stress distribution in the soil under the foundation of the buildings and investigate the efficiency of pounding mitigation procedures taking into consideration SSI effect. In this paper, four cases are studied as follows:

- The effect of pounding on the seismic response of adjacent 4HRBs in terms of lateral displacements, base shear forces, and base moments is studied under different earthquakes considering SSI effect.
- Mitigation of pounding effect by means of connecting the adjacent 4HRBs by FVLs is studied considering SSI effect.
- The influence of improving soil bearing capacity under the foundations of the adjacent 4HRBs on mitigating the pounding effect is also investigated.
- The advantage of using soil improvement procedure along with connecting the adjacent 4HRBs with fluid viscous links to mitigate the pounding effects is inspected.

3. Modeling of the Structural System for Seismic Analysis

To study the seismic response of adjacent buildings, undergo pounding considering SSI effect, three-dimensional model of adjacent 4HRBs group is analysed using SAP2000 program. Each building is twelve storeys with total height of 36 m from ground level with 3 m storey height. The group of buildings consists of four adjacent buildings with two-side projection raft foundations. The

adjacent buildings group induces unequal stresses underneath the foundations due to the difference between the center of gravity of each building and the center of area of its raft foundation. The highest stress point under the foundations appears under the un-projected corner of the raft foundations, as shown in Fig. 1.

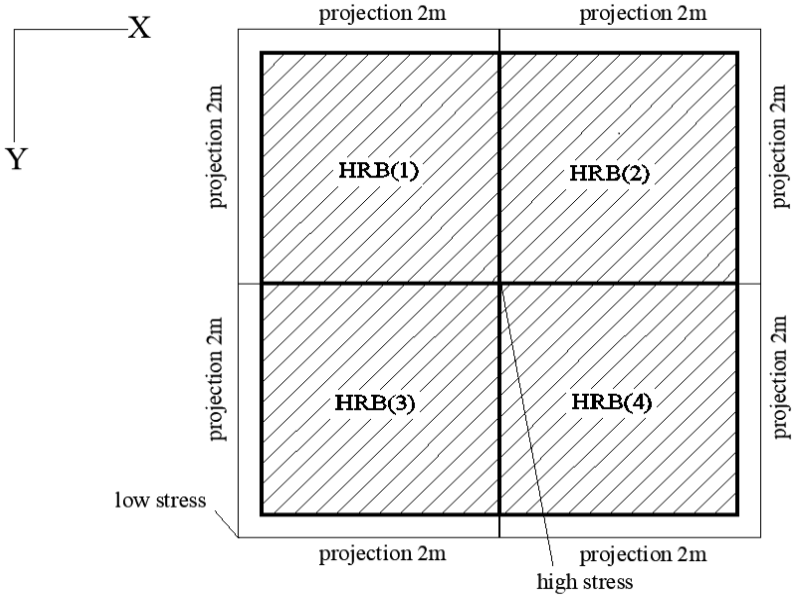

Fig. 1 Group of 4HRBs with 2 m foundation projection (two-side projection of each raft foundation)

3.1. Structural Details of Buildings

Fig. 2 shows detailed structural plans of floor slab and raft foundation of the buildings. Each building is a reinforced concrete structure 20 × 20 m in plan. Buildings are symmetrical in X and Y-direction. A live load for a residential building of 2 kN/m2 is used, while the superimposed dead load is equal to 2 kN/m2. The structural system of each floor consists of slab-beam system with two beam models (b and b1) of 250 × 600 mm in cross-section and spacing 5 m in both directions as shown in Fig. 2(a). Beam b is of 2 Ø12 and 4 Ø16 for top and bottom reinforcement, respectively.

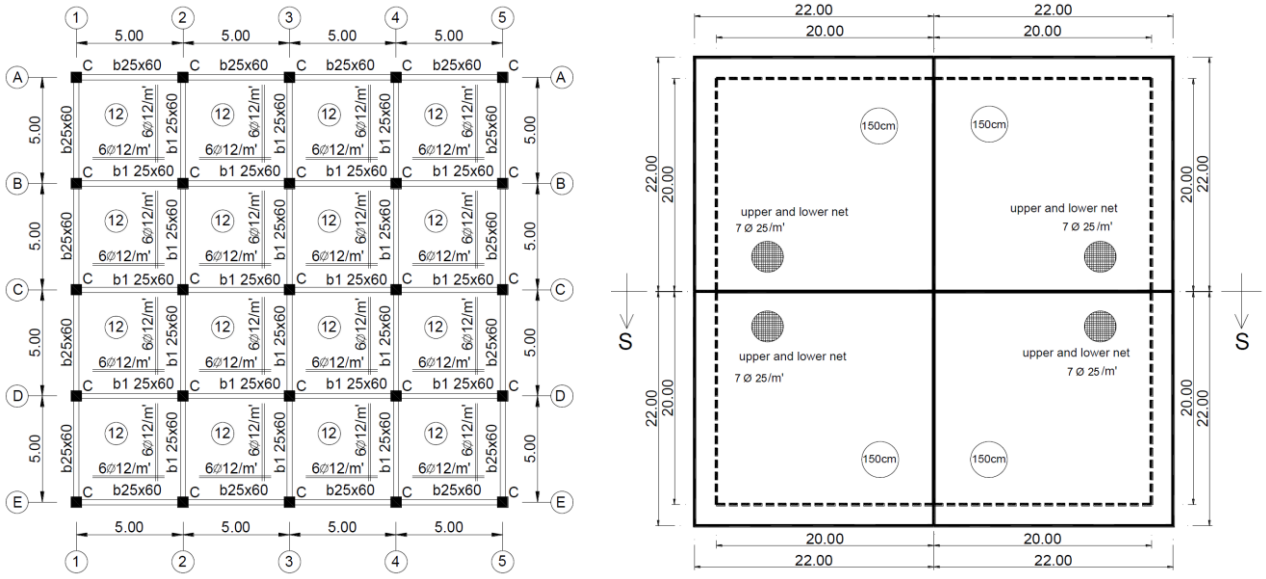

a) Typical structural plan of each floor b) Foundation plan

Fig. 2 Structural plans

For beam b_1, the top and bottom reinforcement are 3 Ø12 and 5 Ø16, respectively. The slab thickness is 120 mm, and the reinforcement is 6 Ø12/m' in each direction. Columns cross section is 800 × 800 mm with reinforcement of 26 Ø18. The raft foundations are of 1500 mm thickness and 7 Ø 25/m' top and bottom mesh as shown in Fig. 2(b). In this paper, the Egyptian Code of Practice (ECP) [33,34] is used. Beams and columns are modelled as frame elements, slabs are defined as shell elements.

3.2. Earthquake Record

Three-dimensional time history analysis is performed using SAP2000 program for four adjacent HRBs with twelve floors heights without a separation gap between buildings large enough to allow individual buildings to vibrate freely. Therefore, pounding occurs, and buildings displacements and storey shears deviate from the no-pounding case. Analysis is performed under four different earthquakes strike in X or Y-direction considering SSI effect. The time history analysis is about 40-s duration and consists of 4000 steps under actual earthquake accelerograms and a vibration segment of 0.01 s duration. The used earthquakes excitations are as shown in Fig. 3. The 1940 El Centro earthquake occurred in the Imperial Valley in south-eastern California with a Magnitude (Mw) = 6.9. The 1995 Kobe earthquake occurred in southern Hyogo prefecture with (Mw) = 6.9. The 1989 Loma Prieta earthquake occurred in northern California with (Mw) = 6.9. The 1994 Northridge earthquake occurred in the San Fernando Valley region of the city of Los Angeles with (Mw) = 6.7. Characteristics of the used ground motions (Magnitude (Mw), Peak Ground Acceleration (PGA), Peak Ground Velocity (PGV), and Epicentral Distance) are given in Table 1.

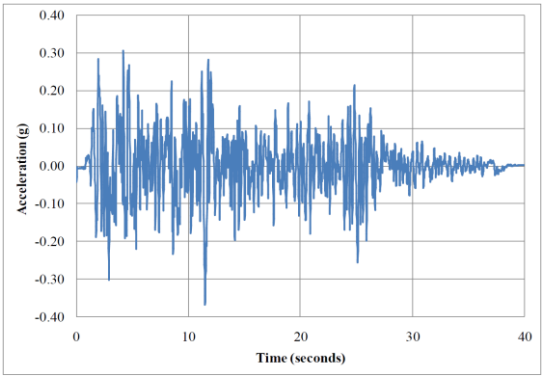

i) El Centro

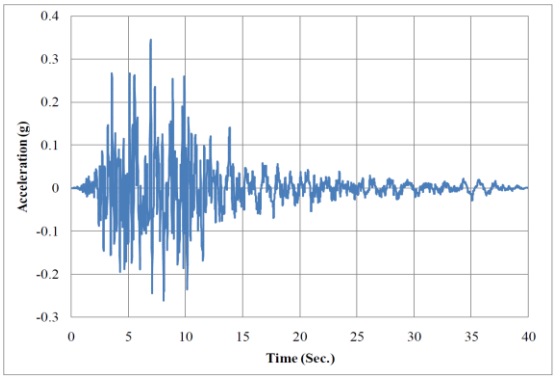

ii) Kobe

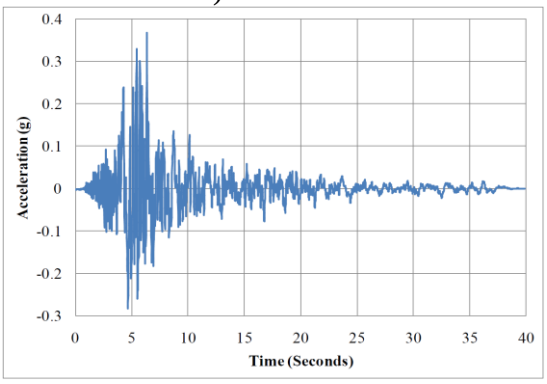

iii) Loma Prieta

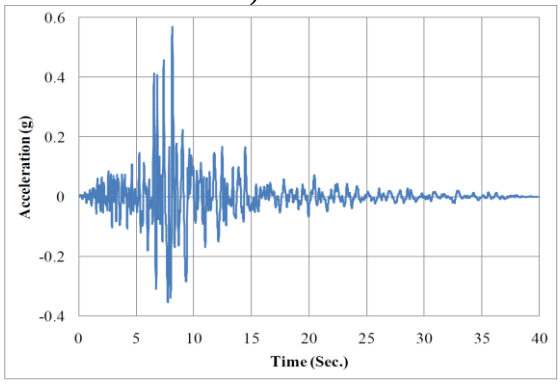

iv) Northridge

Fig. 3 Acceleration signals of used different earthquakes

Table 1: Characteristics of the used ground motions. [35]

Earthquake	Magnitude (Mw)	PGA (g)	PGV (cm/s)	Epi. Dist. (km)
1940 El Centro	6.9	0.37	33.45	12.2
1995 Kobe	6.9	0.345	-	22.5
1989 Loma Prieta	6.9	0.37	62.8	17.2
1994 Northridge	6.7	0.56	51.5	24.1

3.3. Soil-structure Interaction Model

The dynamic characteristics of a structure such as fundamental frequency and vibration modes are dependent on soil stiffness. When the structure is stiff and the underlying soil is soft, the SSI effect becomes important. On the other hand, as the structural period gets longer and the stiffness of the soil under the structure gets higher, SSI loses its importance. In the present study, medium soil is used, the properties of the used soil are shown in Table 2, where, E is the Elastic modulus, G is the strain shear modulus, v is Poisson's ratio, and ρ is the mass density of the soil.

The dynamic model of the foundation-soil interaction system is represented by an equivalent springs and dashpots system in three directions (X, Y, and Z-directions), as shown in Fig. 4. Springs and dashpots represent soil stiffness and soil damping, respectively. The spring stiffness and damping coefficients of the soil in the vertical and horizontal directions for the 3D soil element are calculated using the expressions in Table 3, described by Newmark and Rosenblueth [36]. When a non-circular foundation is considered, an equivalent radius is defined to use these equations. In the present study, the equivalent radius was obtained by equating the area of a circular plate to the square plate and solving for r (Adapted from [37])

Table 2: Soil properties

Soil type	ρ (Mg/m^3)	G (N/mm^2)	v	E (N/mm^2)
Medium	1.95	25	0.4	30

Table 3: Stiffness and damping coefficients of soil model [36].

Direction	Stiffness; k	Damping; c
Vertical	$k = \frac{4Gr}{1-v}$	$c = 1.79\sqrt{k\rho r^3}$
Horizontal	$k = 18.2\,Gr\frac{(1-v^2)}{(2-v)^2}$	$c = 1.08\sqrt{k\rho r^3}$

r = Plate radius; G = shear modulus; v = Poisson's ratio; ρ = mass density.

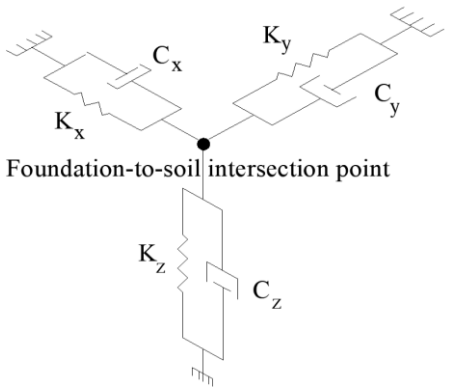

Fig. 4 Soil-foundation interaction element modeled as spring-mass system with viscous damper in three directions

3.4. Impact Elements

In this study, the equivalent impact element of spring-dashpot model is applied to simulate the earthquake-induced pounding between the adjacent buildings. The impact force, $F(t)$, in the model is expressed as [21]:

$$F(t) = k_{imp}\,\delta(t) + c_{imp}\,\dot{\delta}(t) \tag{1}$$

where $\delta(t)$ and $\dot{\delta}(t)$ denote the relative deformation and the relative velocity of the colliding buildings, respectively. k_{imp} is the stiffness of the impact element and c_{imp} is the damping coefficient of the impact element. The value of the damping coefficient of the impact element reflects the energy losses during the inelastic collisions. The coefficient of restitution is utilized for assigning values of the damping coefficient of the impact elements in Anagnostopoulos [38]. If the masses m_1 and m_2 are the masses of the two pounding buildings, then the damping coefficient, c_{imp}, of the impact element in terms of the coefficient of restitution, c_r, is expressed by Anagnostopoulos [38,39] as

$$c_{imp} = 2\zeta\sqrt{k_{imp}\left(\frac{m_1 m_2}{m_1 + m_2}\right)}\ ,\ \zeta = -\frac{lnc_r}{\sqrt{\pi^2 + (lnc_r)^2}} \tag{2}$$

where □ is the damping ratio and lnc_r is the natural logarithm of c_r. Table 4 shows the values of the restitution coefficient c_r via the damping ratio ζ. For concrete-to-concrete impact, as in the application herein, a value of the coefficient of restitution $c_r = 0.65$ is recommended by Jankowski [40], which corresponds to a damping ratio ζ = 0.14.

Table 4: Values of coefficient of restitution (c_r) via damping ratio (ζ).

Case	c_r	ζ
Elastic impact	1	0
Plastic impact	0	1
The study case	0.65	0.14

4. Numerical Results and Discussion

In this section, numerical studies are conducted to examine the mutual effect of pounding between adjacent HRBs due to ground motions in presence of soil stress irregularity taking into consideration SSI effect for more realistic modeling. Furthermore, the effectiveness of proposed pounding mitigation procedures (such as connecting fluid viscous links between buildings and/or improving soil bearing capacity) is investigated. Seismic responses of the pounding adjacent 4HRBs are compared with responses of a single HRB with a two-side projection foundation as a reference case to understand the deviation of the response of pounding HRB from the response of a single HRB under different earthquakes considering SSI. The ratios between the corresponding values of the measured responses are used for the comparison. Additionally, the efficiency of the proposed pounding mitigation procedures is measured by the reduction in the response values of the 4HRBs when applying mitigation procedure relative to the corresponding values of the 4HRBs without mitigation procedures. The studied cases are summarized in Table 5.

Table 5: The studied cases.

Case	Notation	Description
Case1	SC	Single Case (HRB with two-side projection foundation)
Case2	GC1	Group Case1 (Adjacent 4HRBs without mitigation procedure)
Case3	GC2	Group Case2 (Adjacent 4HRBs with soil improvement)
Case4	GC3	Group Case3 (Adjacent 4HRBs connected with fluid viscous links)
Case5	GC4	Group Case4 (Adjacent 4HRBs with soil improvement and fluid viscous links)

4.1 Seismic Response of Adjacent Buildings Subjected to Pounding Considering SSI

To study the effect of seismic-induced pounding between adjacent HRBs in presence of irregular stress distribution in soil, a particular arrangement of adjacent 4HRBs group with two-side projection raft foundation of each building is considered as shown in Fig. 1. The 4HRBs are identical, which means that they have the same dynamic properties and fundamentally will vibrate in-phase in the fixed base cases, which means no collisions will occur. However, in this study, even though the buildings have the same dynamic properties, they vibrated out-of-phase causing collisions. This is apparently due to the consideration of the soil.

Seismic responses for pounding adjacent 4HRBs case (GC1) are inspected along the direction of the ground motion considering the SSI effect. Lateral displacements, base shears, and base moments of the single building case (SC) and of the pounding HRBs case (GC1) are shown in Figs. 5-7. Ratios between maximum lateral displacements, base shears, and base moments of the pounding HRBs case (GC1) and of the single building case (SC) are given in Tables 6-8 for comparison.

Fig. 5 represents the lateral displacements of the single HRB case (SC) and of the pounding HRBs group (GC1) in x and y-directions under different earthquakes considering SSI effect. Fig. 5(a) shows the lateral displacements caused by El Centro earthquake in x and y-directions. The maximum lateral displacement of the HRBs (GC1) records about 0.6 of the corresponding value for the single HRB (SC), as in Table 6. It may be owing to the phenomenon of collision between buildings that leads to the emergence of displacements in opposite directions. Fig. 5(b) shows the lateral displacements caused by Northridge earthquake. The maximum lateral displacement of case (GC1) and of case (SC) have the same value for Northridge earthquake as seen in Table 6. Fig. 5(c) shows the lateral displacements of the buildings subjected to Loma Prieta earthquake. The maximum lateral displacement of case (GC1) records 0.8 of the corresponding value of case (SC). Fig. 5(d) shows the lateral displacements of the buildings subjected to Kobe earthquake. The maximum value of the lateral displacements of case (GC1) is slightly higher than the maximum lateral displacement of case (SC).

Fig. 6 shows the maximum base shear of the buildings in (GC1) and the base shear of the single building (SC) due to the above-mentioned four earthquakes in x and y-directions. Fig. 6(i) represents the base shears in x-direction. It can be noticed from the figure that the maximum base shear in case (GC1) records higher values than the corresponding values in the single building under three of the earthquakes, but the value is lower for the fourth earthquake. Fig. 6(ii) also shows that the values of the maximum base shear in case (GC1) records higher values than that of the single building case in y-direction under the three earthquakes.

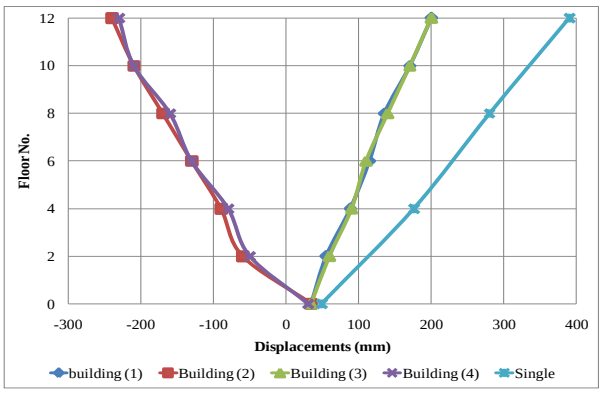

i) X-direction

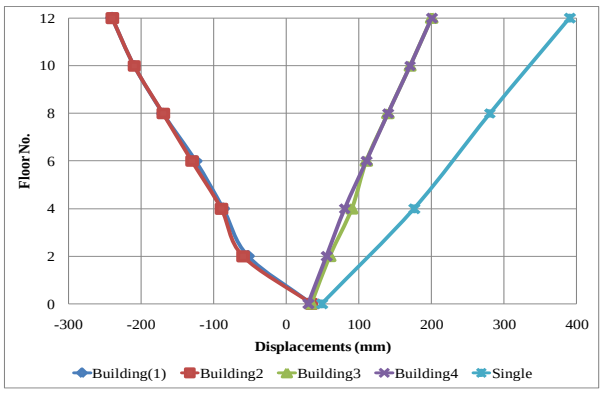

ii) Y-direction

a) El Centro earthquake-lateral displacements (mm)

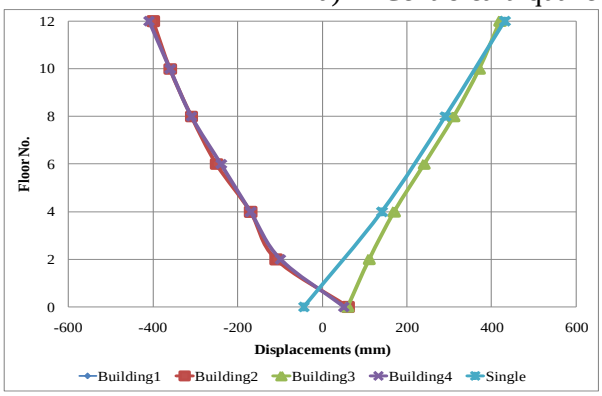

i) X-direction

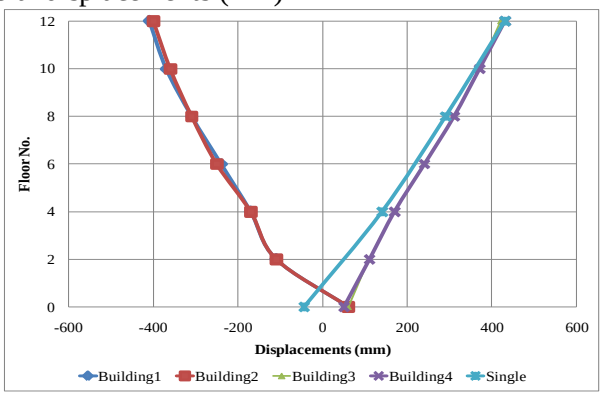

ii) Y-direction

b) Northridge earthquake-lateral displacements (mm)

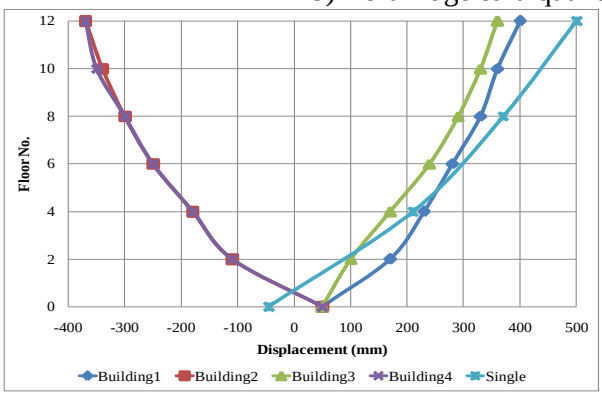

i) X-direction

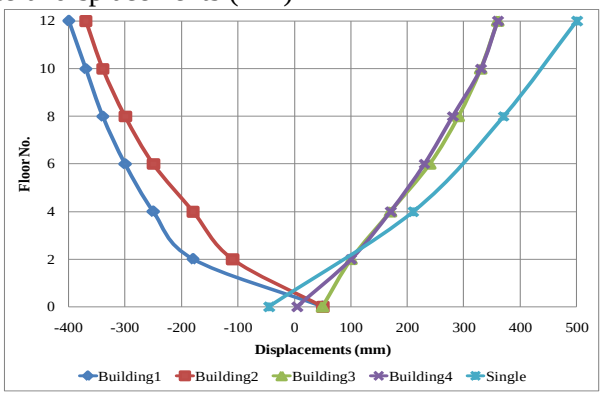

ii) Y-direction

c) Loma Prieta earthquake-lateral displacements (mm)

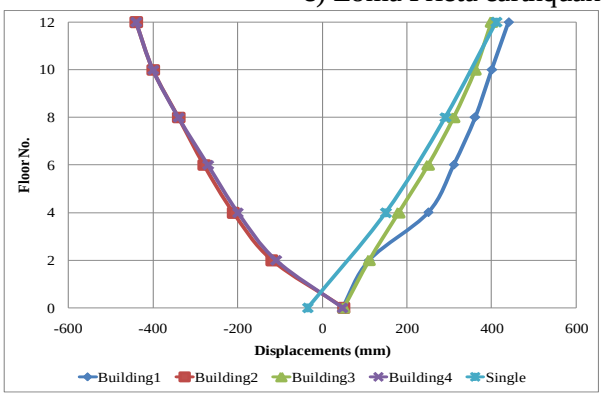

i) X-direction

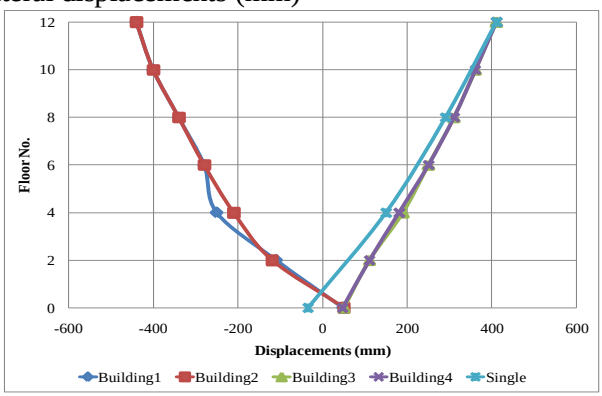

ii) Y-direction

d) Kobe earthquake-lateral displacements (mm)

Fig. 5 Lateral displacements of adjacent 4HRBs without mitigation procedure (GC1) subjected to different earthquakes compared with a single building case (SC) with two-side projection foundation.

Table 6: Maximum lateral displacements of the 4HRBs case without mitigation procedure (GC1) compared with the single case (SC).

Case	Earthquake	Maximum lateral displacements (mm)	Lateral displacements relative to (SC)
SC	El Centro	390	-
	North	430	-
	Loma	500	-
	Kobe	410	-
GC1	El Centro	240	0.6
	North	430	1.0
	Loma	400	0.8
	Kobe	440	1.1

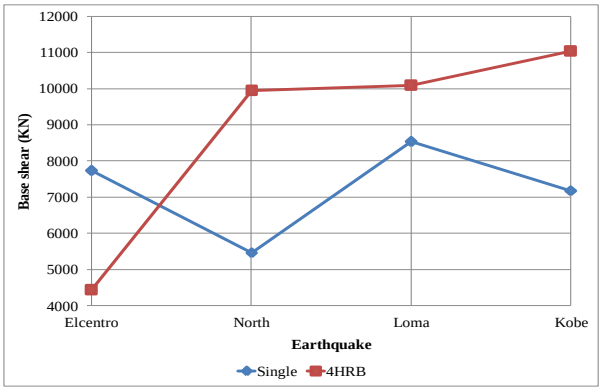

i) x-direction base shear (KN)

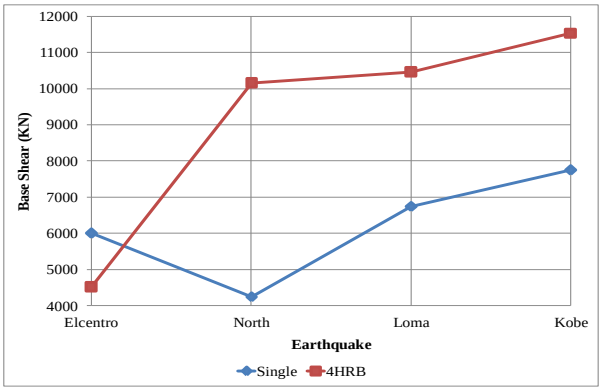

ii) y-direction base shear (KN)

Fig. 6 The maximum base shear of the adjacent 4HRBs without mitigation procedure (GC1) and of the single building case (SC) in x and y-directions.

The maximum values of the base shear for the single case (SC) and for the 4HRBs case without mitigation procedure (GC1) are tabulated in Table 7 for every earthquake. The ratio between the maximum values of the base shear of case (GC1) and the corresponding values of case (SC) is calculated for every earthquake and added in Table 7 in the last column. These ratios range from (0.6 to 1.9), these results indicate that the deviation of the response of pounding HRB from the response of single HRB ranges widely for different earthquakes. Furthermore, in some incidents the response of a pounding HRB is higher than the response of a single HRB, and in other earthquakes is the opposite. In general, earthquakes have different characteristics such as peak acceleration, duration of strong motion, and different ranges of dominant frequencies and therefore have different influences on the structure.

Table 7: Maximum base shear of the 4HRBs case without mitigation procedure (GC1) compared with the single case (SC).

Case	Earthquake	Maximum base shear (KN)	Base shear relative to (SC)
SC	El Centro	7730	-
	North	5470	-
	Loma	8540	-
	Kobe	7750	-
GC1	El Centro	4520	0.6
	North	10150	1.9
	Loma	10460	1.3
	Kobe	11540	1.5

Fig. 7 shows the maximum base moment of the buildings in (GC1) and the base moment of the single building (SC) due to the above-mentioned four earthquakes in x and y-directions. Fig. 7(i) shows that the maximum base moment in case (GC1) records values higher than the corresponding values of the single building in the x-direction under three of the earthquakes, but the value is lower for the fourth earthquake. Fig. 7(ii) shows the base moment in y-direction, it can be seen from the figure that the maximum base moment in (GC1) records values higher than the corresponding values of the single building case under the three earthquakes.

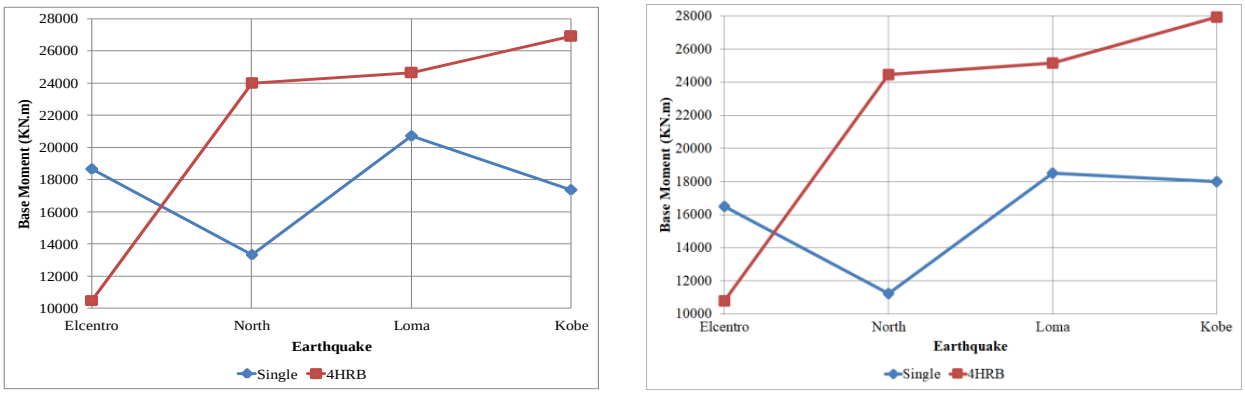

i) x-direction base moment (KN.m) ii) y-direction base moment (KN.m)

Fig. 7 The maximum base moment of the adjacent 4HRBs without mitigation procedure (GC1) and of the single building case (SC) in x and y-directions.

The maximum values of the base moment for the single case (SC) and the maximum values of the base moment for the 4HRBs case without mitigation procedure (GC1) are tabulated in Table 8 for every earthquake. The ratios between the maximum values of the base moment of case (GC1) and the corresponding values of case (SC) are calculated for every earthquake and added in Table 8 in the last column, these ratios range from (0.6 to 1.9). As the base shear, the base moment of the HRB in the group is higher than that of the single HRB in some cases and in other incidents is the opposite.

Table 8: Maximum base moment of the 4HRBs case without mitigation procedure (GC1) compared with the single case (SC).

Case	Earthquake	Maximum base moment (KN.m)	Base moment relative to (SC)
SC	El Centro	18650	-
	North	13310	-
	Loma	20720	-
	Kobe	18000	-
GC1	El Centro	10810	0.6
	North	24480	1.9
	Loma	25160	1.3
	Kobe	27940	1.6

It can be noticed from the above results that the base shears and base moments of the HRBs in group record higher values than the corresponding values of the single building case under most of the considered earthquakes. This may be attributed to the partial restraint in lateral displacements caused by the movement restraint provided by the adjacent buildings. However, the comparison

between the single case (SC) and the pounding case (GC1) has revealed that pounding between adjacent HRBs may not enormously increase the buildings straining actions as base shears and base moments under some earthquakes (as seen in El Centro earthquake instance) despite the less lateral displacement compared to the single case. This is apparently due to the different characteristics of every earthquake.

The effect of using pounding mitigation procedures on the seismic response of adjacent buildings taking into consideration the SSI effect is investigated herein. Three different mitigation procedures are examined to reduce the pounding effect between the adjacent 4HRBs, as follows:

- Improving soil by means of driven piles in the connecting zone between the adjacent 4HRBs under raft foundations (at the highly stressed zone).
- Linking the adjacent 4HRBs by fluid viscous links.
- A combination of the two previous methods.

4.2 Seismic Response of Adjacent Buildings Subjected to Pounding with Soil Improvement

The Soil under the foundations of the adjacent 4HRBs is medium soil with a highly stressed region under the connecting zone of the raft foundations of the buildings. The properties of the used soil are shown in Table 2. Fig. 1 shows the high stress points and the low stress points under the foundations. Increasing the soil bearing capacity in the highly stressed region under the connecting zone may reduce the pounding effect between the adjacent buildings. Driven piles procedure is utilized as a soil improvement technique. Driven piles are used to confine and strengthen the soil to improve the bearing capacity of the soil. In the present study, the spacing-to-pile diameter ratio (S/D) is assigned to be equal to 4. Piles are distributed in a 2 m x 2 m array in half of the area under each raft foundation around the connecting zone between the adjacent 4HRBs as shown in Fig. 8.

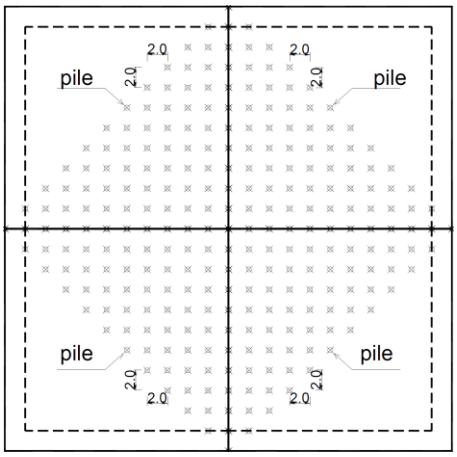

Fig. 8 Piles distribution under half of the raft foundation of each adjacent building.

To investigate the effectiveness of soil improvement on the seismic response of adjacent buildings undergo pounding, the seismic responses of the adjacent 4HRBs with driven piles in the highly stressed soil region are inspected under different earthquakes considering SSI effect. Lateral displacements, base shears, and base moments of the pounding HRBs (GC2) and of the single building (SC) are shown in Figs. 9-11. The responses of the adjacent 4HRBs with soil improvement (GC2) are compared with the responses of the single building (SC) and with the responses of the adjacent 4HRBs without mitigation procedure (GC1) in Tables 9-1.

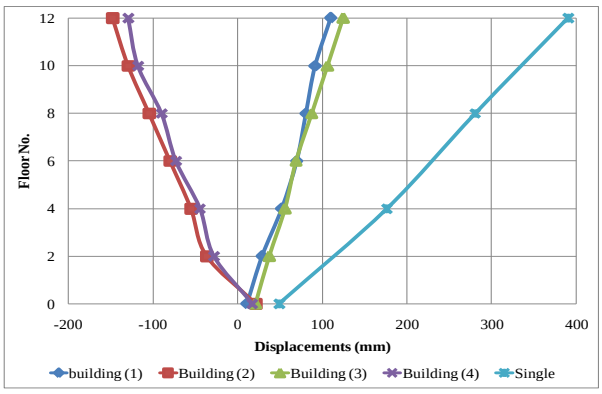

i) X-direction

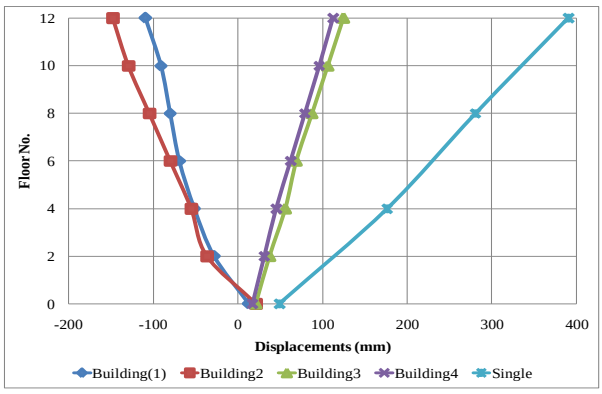

ii) Y-direction

a) El Centro earthquake-lateral displacements (mm)

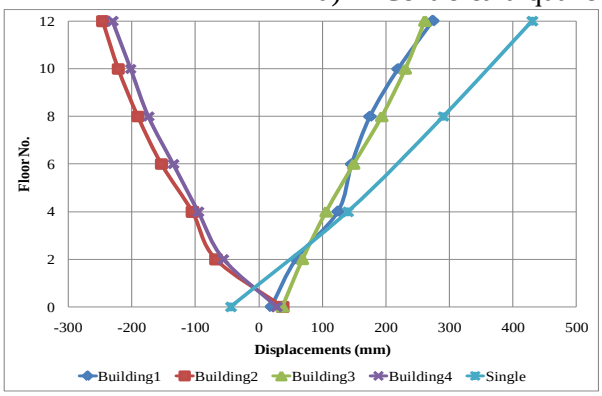

i) X-direction

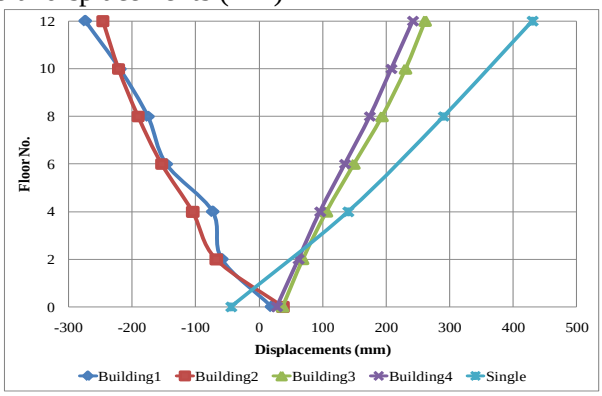

ii) Y-direction

b) Northridge earthquake-lateral displacements (mm)

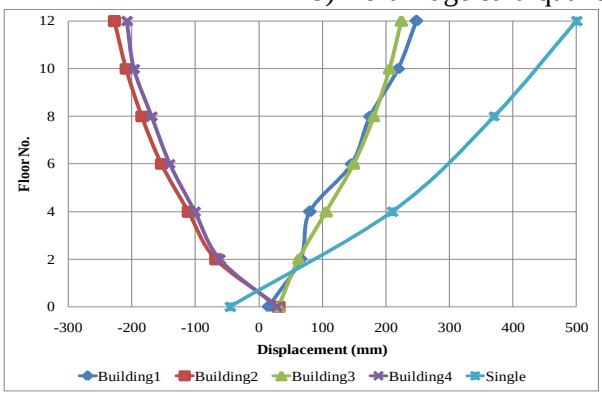

i) X-direction

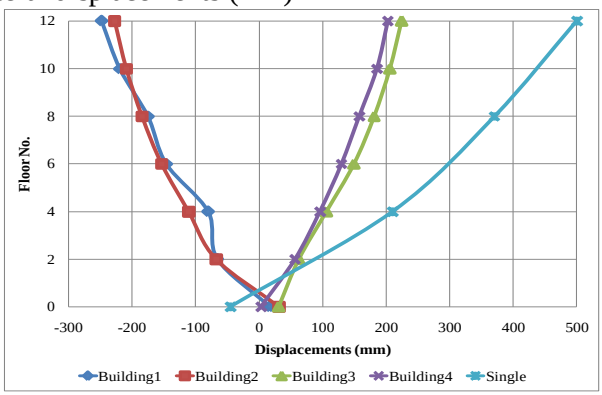

ii) Y-direction

c) Loma Prieta earthquake-lateral displacements (mm)

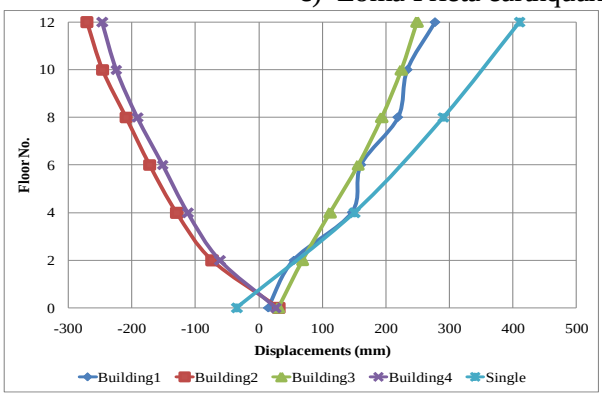

i) X-direction

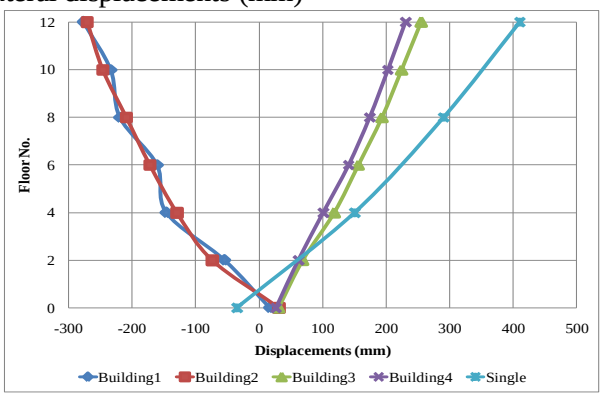

ii) Y-direction

d) Kobe earthquake-lateral displacements (mm)

Fig. 9 Lateral displacements of adjacent 4HRBs with soil improvement (GC2) subjected to different earthquakes compared with a single building case (SC) with two-side projection foundation.

Fig. 9 represents the lateral displacements of the single HRB (SC) and of the pounding HRBs (GC2) in x and y-directions under the four earthquakes considering the SSI effect. Fig. 9(a) shows the lateral displacements caused by El Centro earthquake in x and y-directions. The maximum lateral displacement of the 4HRBs (GC2) records about 0.4 of the corresponding value for the single HRB (SC), as shown in Table 9. Fig. 9(b) shows the lateral displacements caused by Northridge earthquake. The maximum lateral displacement of (GC2) records about 0.6 of the corresponding value of (SC), as seen in Table 9. Fig. 9(c) shows the lateral displacements of the buildings subjected to Loma Prieta earthquake. The maximum lateral displacement of case (GC2) is 0.5 of the corresponding value of case (SC). Fig. 9(d) shows the lateral displacements of the buildings subjected to Kobe earthquake. The maximum value of the lateral displacements of case (GC2) is 0.7 of the maximum lateral displacement of case (SC), as shown in Table 9. The reduction in the lateral displacements of case (GC2) relative to case (GC1) ranges from 37% to 42% as shown in Table 9. These results suggest that increasing soil bearing capacity generally governs the response of adjacent buildings exposed to seismic-induced pounding.

Table 9: Maximum lateral displacements of the 4HRBs case with soil improvement (GC2) compared with the single case (SC) and with the 4HRBs case without mitigation procedure (GC1).

Case	Earthquake	Maximum lateral displacements (mm)	Lateral displacements relative to (SC)	Lateral displacements reduction relative to (GC1)
SC	El Centro	390	-	-
	North	430	-	-
	Loma	500	-	-
	Kobe	410	-	-
GC1	El Centro	240	0.6	-
	North	430	1.0	-
	Loma	400	0.8	-
	Kobe	440	1.1	-
GC2	El Centro	140	0.4	42%
	North	270	0.6	38%
	Loma	240	0.5	40%
	Kobe	280	0.7	37%

Fig. 10 shows the maximum base shear of the buildings in (GC2) and the base shear of the single building (SC) due to the above-mentioned four earthquakes in x and y-directions. Table 10 contains the maximum value of the base shear for case (SC), case (GC1), and case (GC2) for every earthquake. It can be noticed that the maximum base shear of case (GC2) records higher values than the corresponding values of case (SC) in some incidents, and the value is lower in other incidents. But, in general, the deviation of the values of case (GC2) from the values of case (SC) is less than the deviation found between the values of case (GC1) and case (SC), as can be noticed from the calculated values of the base shear relative to (SC) in Table 10. The ratios between the maximum values of the base shear of (GC1) and (SC) range from (0.6 to 1.9). However, the ratios between the maximum values of (GC2) and (SC) range from (0.5 to 1.5), as given in Table 10.

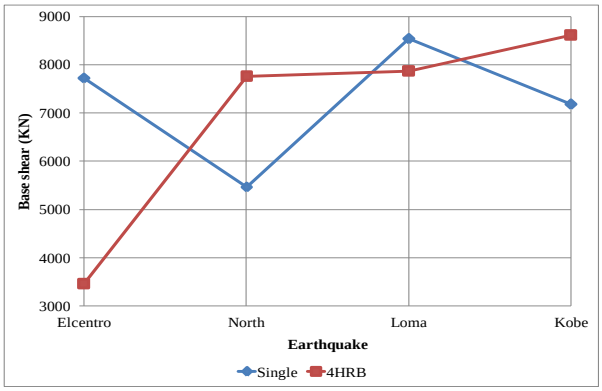

i) x-direction base shear (KN)

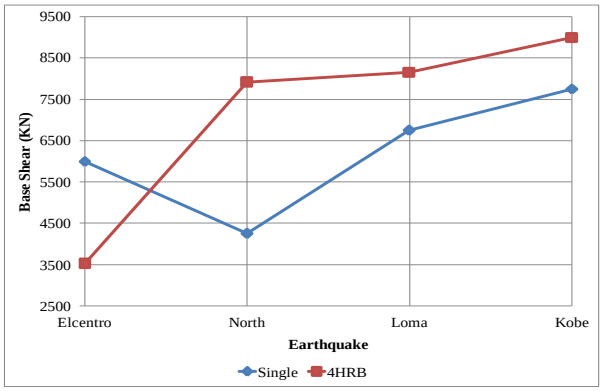

ii) y-direction base shear (KN)

Fig. 10 The maximum base shear of the adjacent 4HRBs with soil improvement (GC2) and of the single building case (SC) in x and y-directions.

Table 10: Maximum base shear of the 4HRBs case with soil improvement (GC2) compared with the single case (SC) and with the 4HRBs case without mitigation procedure (GC1).

Case	Earthquake	Maximum base shear (KN)	Base shear relative to (SC)	Base shear reduction relative to (GC1)
SC	El Centro	7730	-	-
	North	5470	-	-
	Loma	8540	-	-
	Kobe	7750	-	-
GC1	El Centro	4520	0.6	-
	North	10150	1.9	-
	Loma	10460	1.3	-
	Kobe	11540	1.5	-
GC2	El Centro	3560	0.5	22%
	North	7920	1.5	22%
	Loma	8150	1	23%
	Kobe	8970	1.2	23%

Fig. 11 shows the maximum base moment of (GC2) and the base moment of (SC) due to the four earthquakes in x and y-directions. The base moment of case (GC2) records higher values than the corresponding values of case (SC) in some incidents. However, it can be noticed from Fig. 11 that the deviation of the base moment of case (GC2) from case (SC) is less than the deviation found for case (GC1). The ratios between the maximum values of base moment for both case (GC1) and case (GC2) corresponding to the values of case (SC) are calculated for every earthquake and added in Table 11 on the last column.

Furthermore, the reduction in the values of the maximum base shear of case (GC2) relative to case (GC1) is provided in Table 10, and the reduction in the values of the maximum base moment of case (GC2) relative to case (GC1) is provided in Table 11 to discuss the efficiency of this mitigation procedure. It is found that the lateral displacements, the maximum base shears, and the maximum base moments of case (GC2) record values less than the corresponding values of case (GC1) under all the considered earthquakes. The reduction in the lateral displacements of case (GC2) relative to case (GC1) is (37- 42%). The reduction in maximum base shear of case (GC2) relative to case (GC1) is (22-23%). The reduction in the maximum base moment of case (GC2) relative to case

(GC1) is (25-26%) under the considered earthquakes, see Tables 9-11. These results imply the effectiveness of the proposed soil improvement technique with driven piles as a procedure to mitigate the effect of pounding.

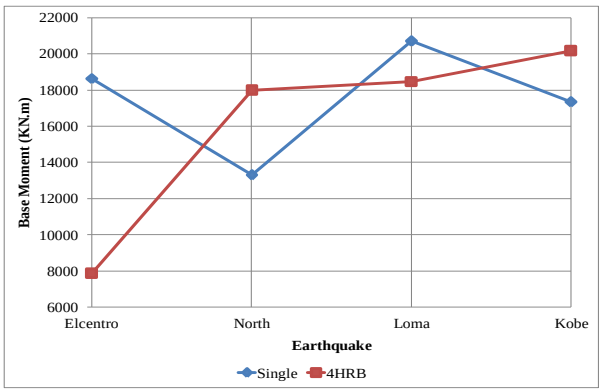

i) x-direction base moment (KN.m)

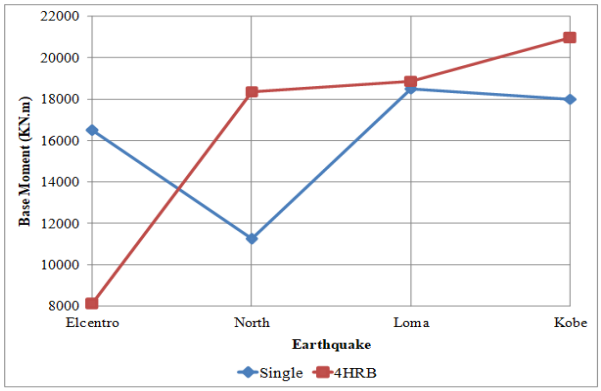

ii) y-direction base moment (KN.m)

Fig. 11 The maximum base moment of the adjacent 4HRBs with soil improvement (GC2) and of the single building case (SC) in x and y-directions.

Table 11: Maximum base moment of the 4HRBs case with soil improvement (GC2) compared with the single case (SC) and with the 4HRBs case without mitigation procedure (GC1).

Case	Earthquake	Maximum base moment (KN.m)	Base moment relative to (SC)	Base moment reduction relative (GC1)
SC	El Centro	18650	-	-
	North	13310	-	-
	Loma	20720	-	-
	Kobe	18000	-	-
GC1	El Centro	10810	0.6	-
	North	24480	1.9	-
	Loma	25160	1.3	-
	Kobe	27940	1.6	-
GC2	El Centro	8100	0.5	26%
	North	18350	1.4	26%
	Loma	18950	1	25%
	Kobe	21050	1.2	25%

4.3 Seismic Response of Adjacent Buildings Subjected to Pounding and Linked with FVLs

Mitigation of pounding effects by means of applying fluid viscous links between adjacent buildings is a well-known technique. In this research, the seismic response of the adjacent 4HRBs linked with FVLs is investigated considering the SSI effect. Results are utilized to compare the efficiency of improving soil bearing capacity and / or applying FVLs procedures in mitigating the combined effects of collision and soil stress irregularity on the seismic response of adjacent buildings. FVLs are distributed between the adjacent 4HRBs as shown in Fig. 12 to mitigate the effect of pounding between the adjacent 4HRBs.

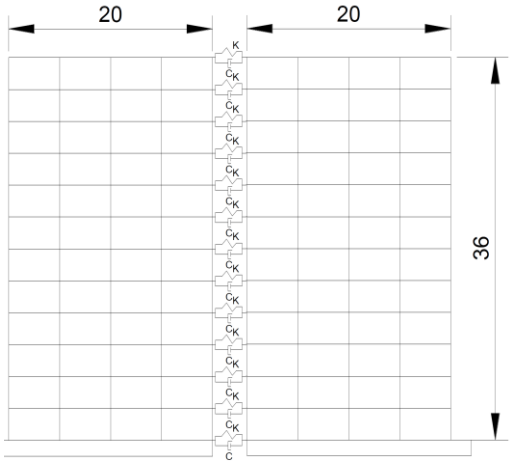

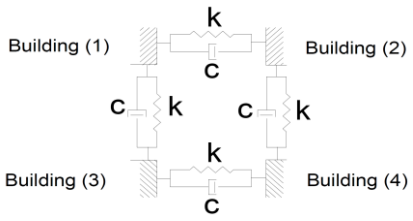

i) FVLs placements over the height of the four buildings ii) FVLs between the four buildings in plan

Fig. 12 Distribution of Fluid Viscous Links (FVLs) in elevation and in plan between the 4HRBs.

Fig. 13 represents the lateral displacements of the adjacent 4HRBs linked with FVLs (GC3) and of the single HRB (SC) in x and y-directions under different earthquakes considering the SSI effect. Table 12 contains the ratios between the values of the maximum lateral displacements of (GC3) and the corresponding values of (SC) for comparison. The maximum lateral displacement of case (GC3), caused by El Centro earthquake, records about 0.2 of the corresponding value of case (SC) as in Table 12. The maximum lateral displacement of case (GC3) relative to that of case (SC) is 0.3 for Northridge earthquake as seen in Table 12. The maximum lateral displacement of case (GC3), subjected to Loma Prieta earthquake, records 0.3 of the corresponding value of case (SC). The maximum value of the lateral displacements of case (GC3) subjected to Kobe earthquake is 0.4 of the maximum lateral displacement of case (SC). The reduction in lateral displacements of case (GC3) relative to case (GC1) ranges from 68% to 71% as shown in Table 12. These results verify that connecting adjacent HRBs with fluid viscous links enormously reduces the lateral displacements of such buildings even in presence of the combined effects of collision and soil stress irregularity.

Table 12: Maximum lateral displacements of the 4HRBs case connected with fluid viscous links (GC3) compared with the single case (SC) and with the 4HRBs case without mitigation procedure (GC1).

Case	**Earthquake**	**Maximum lateral displacements (mm)**	**Lateral displacements relative to (SC)**	**Lateral displacements reduction relative to (GC1)**
SC	El Centro	390	-	-
	North	430	-	-
	Loma	500	-	-
	Kobe	410	-	-
GC1	El Centro	240	0.6	-
	North	430	1.0	-
	Loma	400	0.8	-
	Kobe	440	1.1	-
GC3	El Centro	70	0.2	71%
	North	140	0.3	68%
	Loma	130	0.3	68%
	Kobe	140	0.4	69%

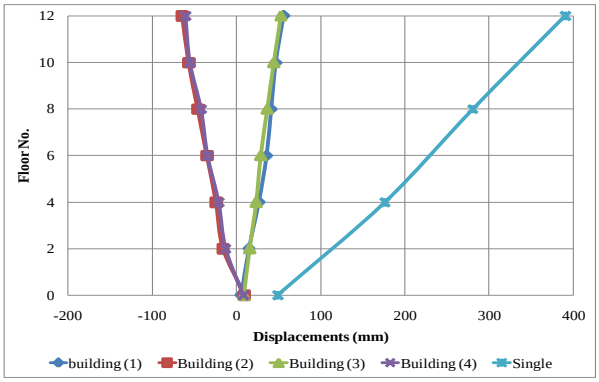

i) X-direction

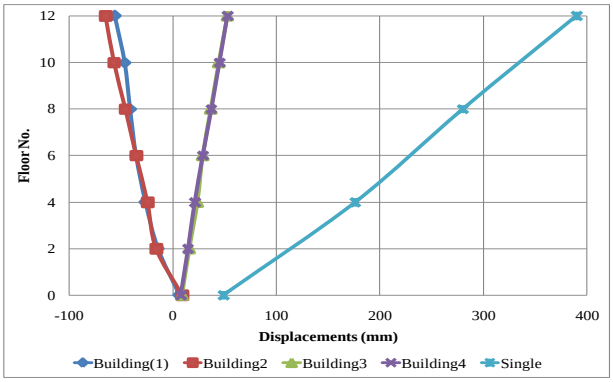

ii) Y-direction

a) El Centro earthquake-lateral displacements (mm)

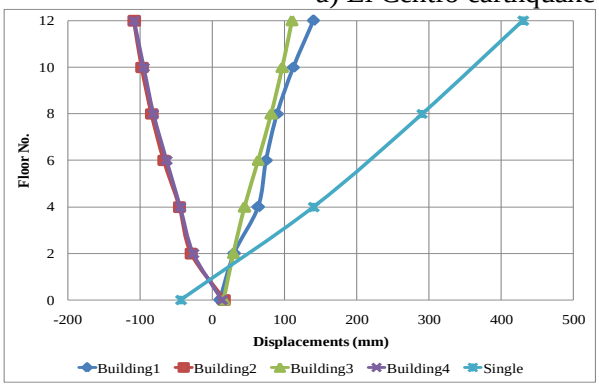

i) X-direction

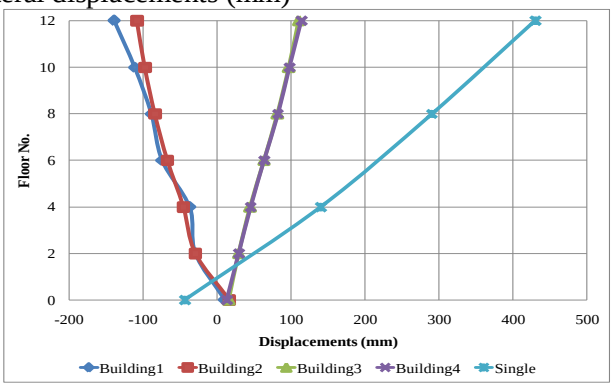

ii) Y-direction

b) Northridge earthquake-lateral displacements (mm)

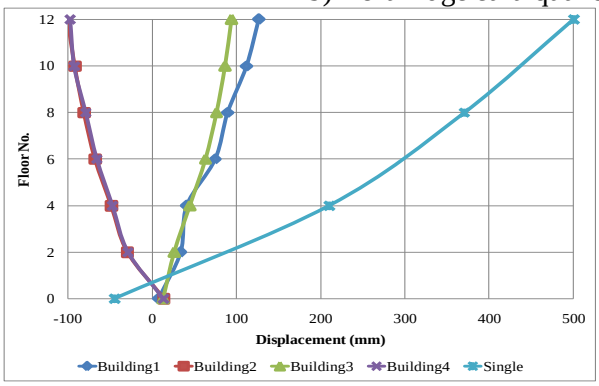

i) X-direction

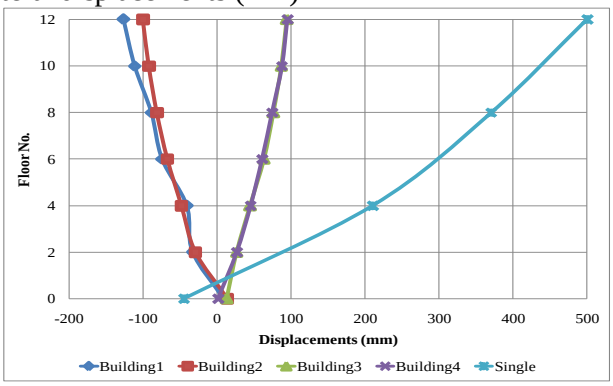

ii) Y-direction

c) Loma Prieta earthquake-lateral displacements (mm)

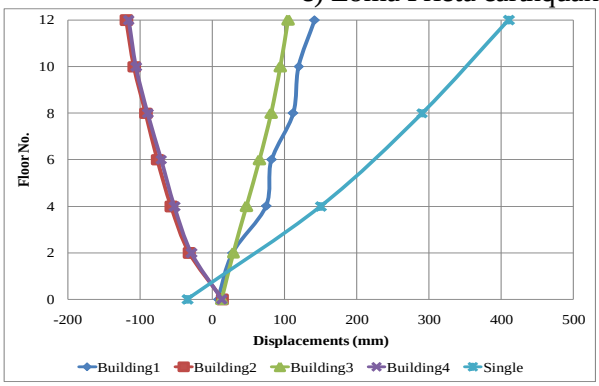

i) X-direction

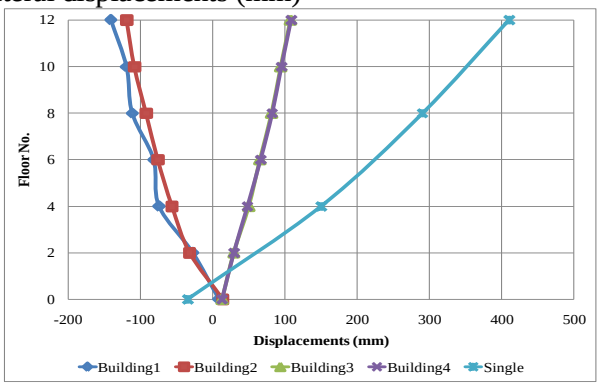

ii) Y-direction

d) Kobe earthquake-lateral displacements (mm)

Fig. 13 Lateral displacements of adjacent 4HRBs connected with fluid viscous links (GC3) subjected to different earthquakes compared with a single building case (SC) with two-side projection foundation.

Fig. 14 shows the maximum base shear of the buildings in case (GC3) and the base shear of case (SC) due to the four earthquakes in x and y-directions. It can be seen from Fig. 14 that the maximum base shear in case (GC3) is lower than the corresponding values in (SC) in most incidents. Table 13 contains the maximum values of the base shear for case (SC), case (GC1), and case (GC3) for every earthquake. The ratios between the maximum values of the base shear of (GC1) and (SC) range from (0.6 to 1.9). However, these ratios between (GC3) and (SC) range from (0.4 to 1.1), as given in Table 13. Furthermore, the reduction in the maximum base shear of case (GC3) is 45% relative to case (GC1), as provided in Table 13.

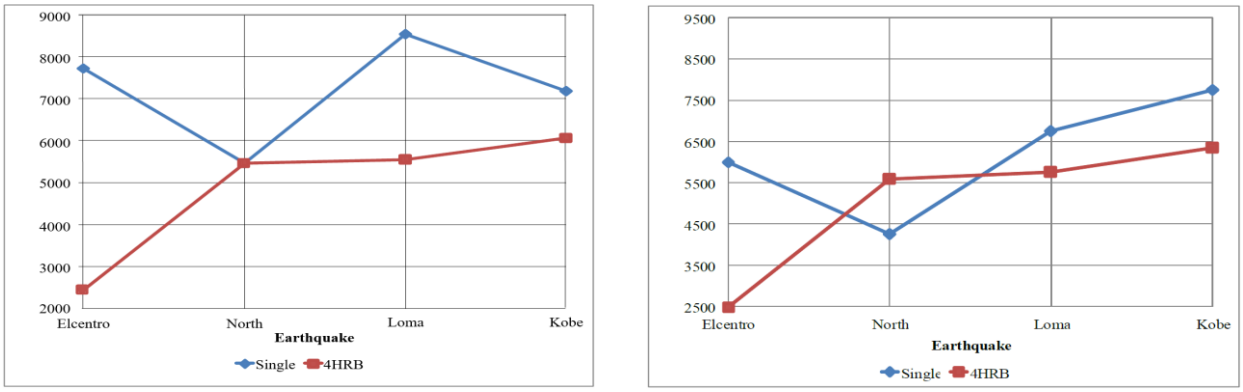

i) x-direction base shear (KN) ii) y-direction base shear (KN)

Fig. 14 The maximum base shear of the adjacent 4HRBs connected with fluid viscous links (GC3) and of the single building case (SC) in x and y-directions.

Table 13: Maximum base shear of the 4HRBs case connected with fluid viscous links (GC3) compared with the single case (SC) and with the 4HRBs case without mitigation procedure (GC1).

Case	Earthquake	Maximum base shear (KN)	Base shear relative to (SC)	Base shear reduction relative to (GC1)
SC	El Centro	7730	-	-
	North	5470	-	-
	Loma	8540	-	-
	Kobe	7750	-	-
GC1	El Centro	4520	0.6	-
	North	10150	1.9	-
	Loma	10460	1.3	-
	Kobe	11540	1.5	-
GC3	El Centro	2490	0.4	45%
	North	5600	1.1	45%
	Loma	5770	0.7	45%
	Kobe	6380	0.9	45%

Fig. 15 shows the maximum base moment of case (GC3) and the base moment of case (SC). Table 14 contains the maximum values of the base moment for case (SC), case (GC1), and case (GC3) for every earthquake. The ratios between the maximum values of the base moment of (GC1) and (SC) range from (0.6 to 1.9). However, the ratios between the maximum values of (GC3) and (SC) range from (0.4 to 1.2). However, the reduction in the base moment of case (GC3) relative to case (GC1) ranges from (38% to 39%), as given in Table 14. Thus, connecting HRBs with fluid viscous links in presence of the combined effects of the collision and the soil stress irregularity not only reduces

lateral displacements but also highly mitigates the other seismic responses as base shears and moments.

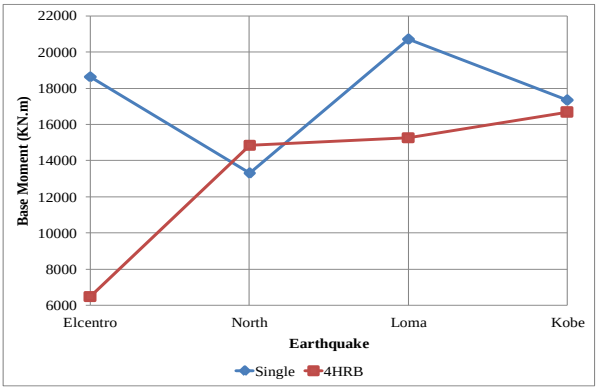

i) x-direction base moment (KN.m)

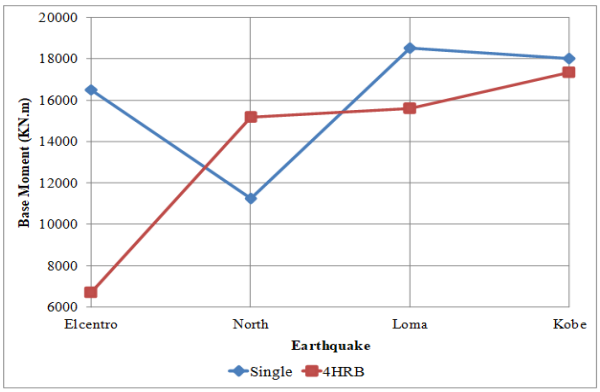

ii) y-direction base moment (KN.m)

Fig. 15 The maximum base moment of the adjacent 4HRBs connected with fluid viscous links (GC3) and of the single building case (SC) in x and y-directions.

Table 14: Maximum base moment of the 4HRBs case connected with fluid viscous links (GC3) compared with the single case (SC) and with the 4HRBs case without mitigation procedure (GC1).

Case	Earthquake	Maximum base moment (KN.m)	Base moment relative to (SC)	Base moment reduction relative to (GC1)
SC	El Centro	18650	-	-
	North	13310	-	-
	Loma	20720	-	-
	Kobe	18000	-	-
GC1	El Centro	10810	0.6	-
	North	24480	1.9	-
	Loma	25160	1.3	-
	Kobe	27940	1.6	-
GC3	El Centro	6750	0.4	38%
	North	15250	1.2	38%
	Loma	15700	0.8	38%
	Kobe	17250	1	39%

4.4 Seismic Response of Adjacent Buildings Subjected to Pounding and Linked with FVLs in Presence of Soil Improvement Procedure

The integration between improving soil bearing capacity and connecting adjacent buildings with FVLs is proposed herein to control the seismic response of buildings that impose irregular soil stress and undergo pounding. The procedure suggested in Fig. 8 to improve soil bearing capacity under the 4HRBs is applied in addition to connecting the 4HRBs with FVLs as shown in Fig. 12. The seismic responses of the adjacent 4HRBs (GC4) considering this integration procedure are introduced in Figs. 16-18 and Tables 15-17. Figs. 16(a-d) represents the lateral displacements of case (GC4) and case (SC) subjected to El Centro, Northridge, Loma Prieta, and Kobe earthquakes, respectively, considering SSI effect.

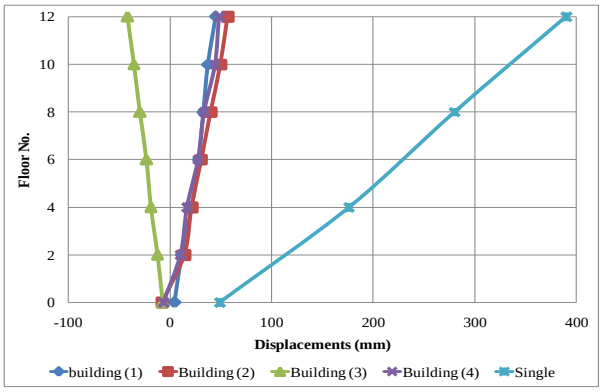

i) X-direction

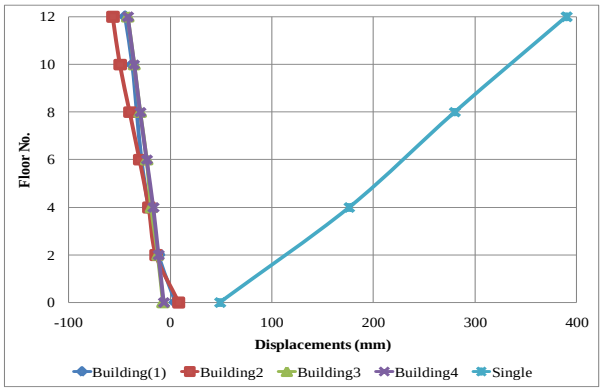

ii) Y-direction

a) El Centro earthquake-lateral displacements (mm)

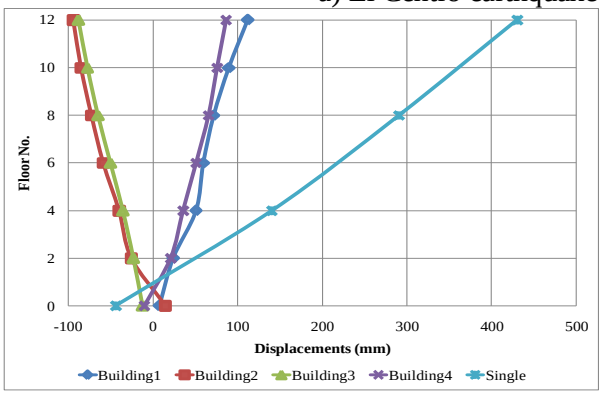

i) X-direction

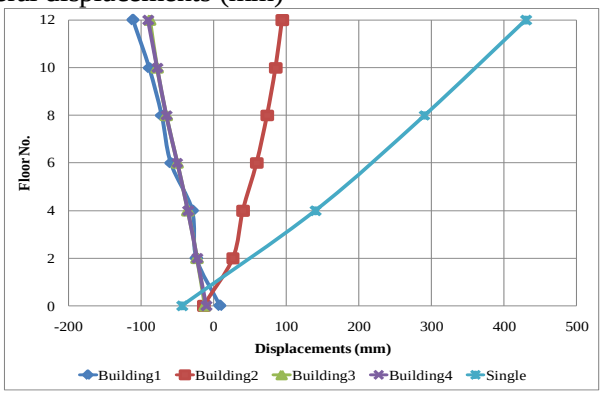

ii) Y-direction

b) Northridge earthquake-lateral displacements (mm)

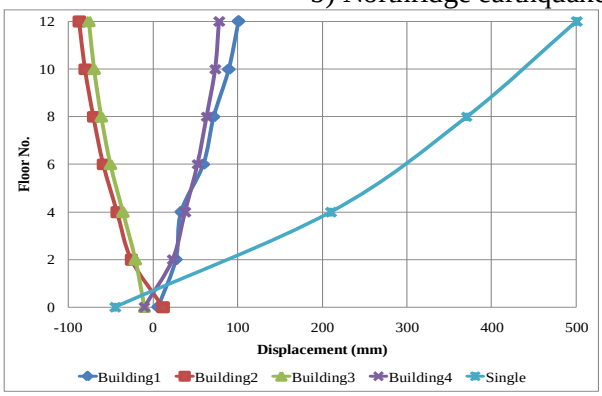

i) X-direction

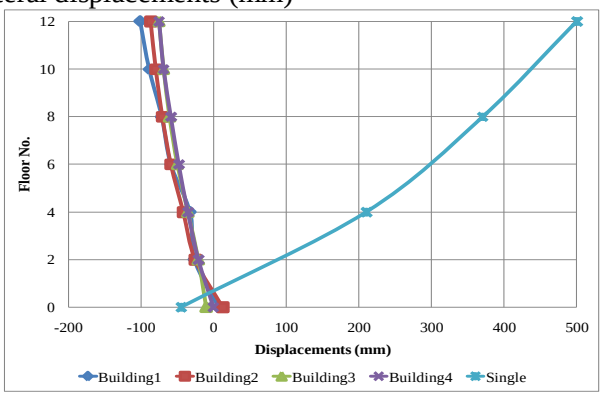

ii) Y-direction

c) Loma Prieta earthquake-lateral displacements (mm)

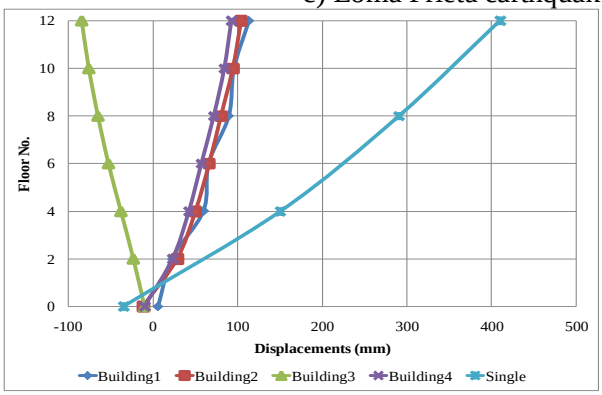

i) X-direction

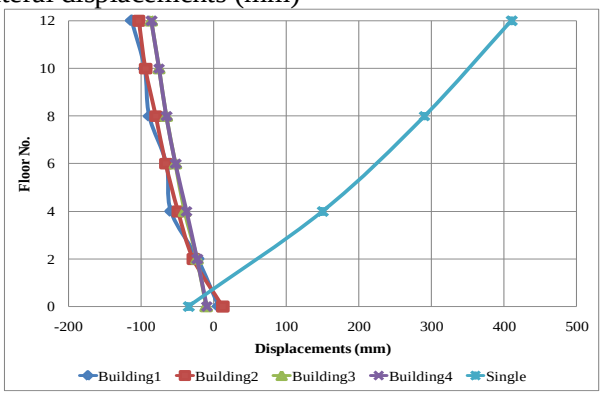

ii) Y-direction

d) Kobe earthquake-lateral displacements (mm)

Fig. 16 Lateral displacements of adjacent 4HRBs with soil improvement and connected with fluid viscous links (GC4) subjected to different earthquakes compared with a single building case (SC) with two-side projection foundation.

Table 15 includes the ratios of the maximum lateral displacements of (GC4) and (GC1) to (SC) and the reduction in the maximum lateral displacements of case (GC4) relative to case (GC1) for the four earthquakes. The maximum lateral displacement of case (GC4) subjected to El Centro earthquake records about 0.2 of the corresponding value for case (SC) as stated in Table 15. The maximum lateral displacement of (GC4) subjected to Northridge earthquake records about 0.3 of the corresponding value for (SC). The maximum lateral displacement of case (GC4) subjected to Loma Prieta earthquake is 0.2 of the corresponding value of case (SC). The maximum value of the lateral displacements of case (GC4) subjected to Kobe earthquake is 0.3 of the maximum lateral displacement of case (SC). The maximum lateral displacements reduction of case (GC4) relative to case (GC1) ranges from 73% to 75%, as shown in Table 15, while the reduction in the maximum lateral displacements of case (GC3) relative to case (GC1) ranges from 68% to 71% as shown in Table 12. Thus, improving soil bearing capacity along with connecting buildings with FVLs has an advantage over using FVLs only in reducing lateral displacements of adjacent HRBs exposed to seismic-induced pounding.

Table 15: Maximum lateral displacements of the 4HRBs case with soil improvement and connected with fluid viscous links (GC4) compared with the single case (SC) and with the 4HRBs case without mitigation procedure (GC1).

Case	Earthquake	Maximum lateral displacements (mm)	Lateral displacements relative to (SC)	Lateral displacements reduction relative to (GC1)
SC	El Centro	390	-	-
	North	430	-	-
	Loma	500	-	-
	Kobe	410	-	-
GC1	El Centro	240	0.6	-
	North	430	1.0	-
	Loma	400	0.8	-
	Kobe	440	1.1	-
GC4	El Centro	60	0.2	75%
	North	110	0.3	75%
	Loma	100	0.2	75%
	Kobe	120	0.3	73%

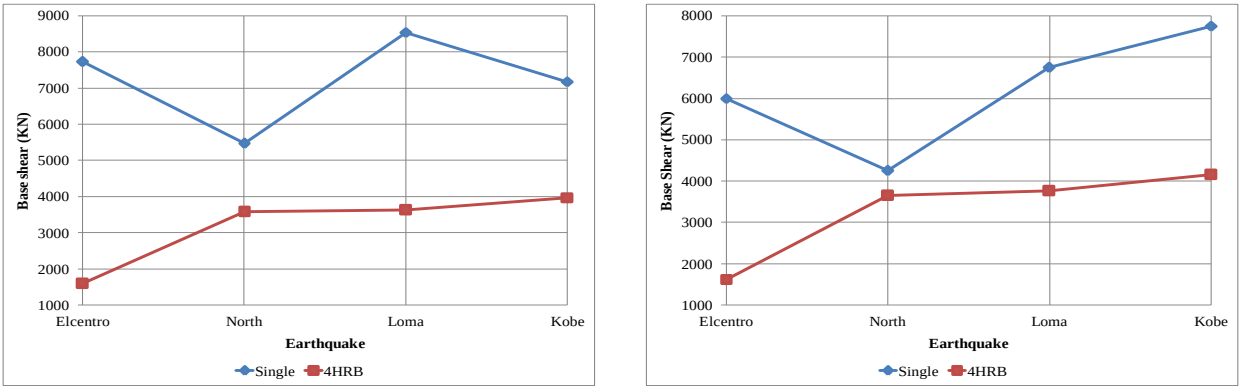

i) x-direction base shear (KN) ii) y-direction base shear (KN)

Fig. 17 The maximum base shear of the adjacent 4HRBs with soil improvement and connected with fluid viscous links (GC4) and of the single building case (SC) in x and y-directions.

Fig. 17 shows the maximum base shear of case (GC4) and the base shear of case (SC). The values of the maximum base shear of case (GC4) are significantly lower than the corresponding values of case (SC), see Fig. 17. The ratios between the maximum values of the base shear of (GC4) and (SC) ranges from (0.3 to 0.7). Furthermore, the reduction in values of the maximum base shear of case (GC4) relative to case (GC1) ranges from 64% to 65% as stated in Table 16. Fig. 18 shows the maximum base moment of case (GC4) and the base moment of case (SC). Also, the values of the maximum base moment of case (GC4) are considerably lower than the corresponding values of case (SC), see Fig. 18. The ratios between the maximum values of the base moment of (GC4) and (SC) range from (0.3 to 0.9). Moreover, the reduction in the maximum values of the base moment of case (GC4) relative to case (GC1) ranges from 56% to 57% as stated in Table 17. Results indicate that improving soil bearing capacity alongside with connecting adjacent high-rise buildings with FVLs not only mitigates the pounding effects in terms of reducing the lateral displacements demand of buildings, but also significantly decreases the values of base shears and base moments in adjacent high-rise buildings.

Table 16: Maximum base shear of the 4HRBs case with soil improvement and connected with fluid viscous links (GC4) compared with the single case (SC) and with the 4HRBs case without mitigation procedure (GC1).

Case	Earthquake	Maximum base shear (KN)	Base shear relative to (SC)	Base shear reduction relative to (GC1)
SC	El Centro	7730	-	-
	North	5470	-	-
	Loma	8540	-	-
	Kobe	7750	-	-
GC1	El Centro	4520	0.6	-
	North	10150	1.9	-
	Loma	10460	1.3	-
	Kobe	11540	1.5	-
GC4	El Centro	1640	0.3	64%
	North	3650	0.7	65%
	Loma	3780	0.5	64%
	Kobe	4180	0.6	64%

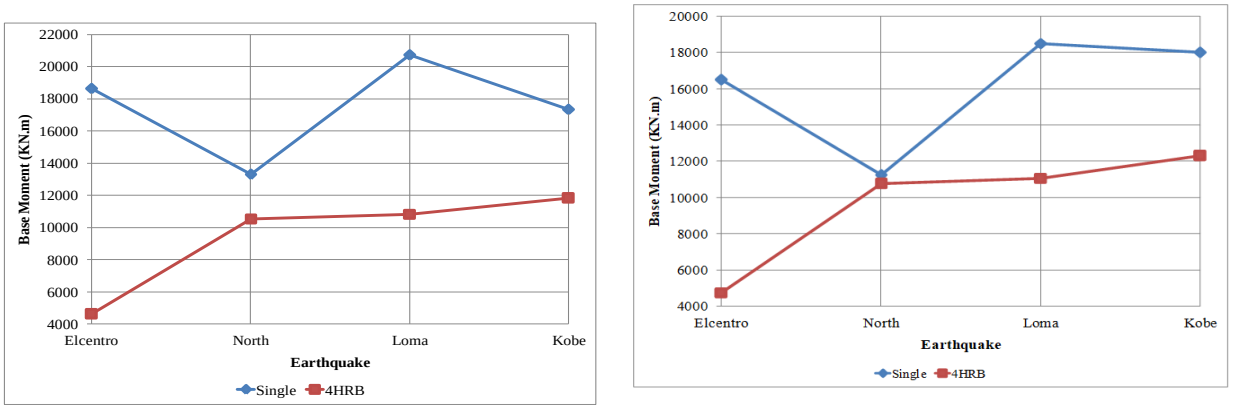

i) x-direction base moment (KN.m) ii) y-direction base moment (KN.m)

Fig. 18 The maximum base moment of the adjacent 4HRBs with soil improvement and connected with fluid viscous links (GC4) and of the single building case (SC) in x and y-directions.

Table 17: Maximum base moment of the 4HRBs case with soil improvement and connected with fluid viscous links (GC4) compared with the single case (SC) and with the 4HRBs case without mitigation procedure (GC1).

Case	Earthquake	Maximum base moment (KN.m)	Base moment relative to (SC)	Base moment reduction relative to (GC1)
SC	El Centro	18650	-	-
	North	13310	-	-
	Loma	20720	-	-
	Kobe	18000	-	-
GC1	El Centro	10810	0.6	-
	North	24480	1.9	-
	Loma	25160	1.3	-
	Kobe	27940	1.6	-
GC4	El Centro	4720	0.3	57%
	North	10800	0.9	56%
	Loma	11100	0.6	56%
	Kobe	12250	0.7	57%

Table 18: Summary of maximum seismic responses of cases (GC2), (GC3), and (GC4) compared with (SC) and (GC1) (Extracted from Tables (9-17)

		Maximum lateral displacements		Maximum base shear		Maximum base moment	
Case	Earthquake	relative to (SC)	reduction relative to (GC1)	relative to (SC)	reduction relative to (GC1)	relative to (SC)	reduction relative to (GC1)
GC1	El Centro	0.6	-	0.6	-	0.6	-
	North	1	-	1.9	-	1.9	-
	Loma	0.8	-	1.3	-	1.3	-
	Kobe	1.1	-	1.5	-	1.6	-
GC2	El Centro	0.4	42%	0.5	22%	0.5	26%
	North	0.6	38%	1.5	22%	1.4	26%
	Loma	0.5	40%	1	23%	1	25%
	Kobe	0.7	37%	1.2	23%	1.2	25%
GC3	El Centro	0.2	71%	0.4	45%	0.4	38%
	North	0.3	68%	1.1	45%	1.2	38%
	Loma	0.3	68%	0.7	45%	0.8	38%
	Kobe	0.4	69%	0.9	45%	1	39%
GC4	El Centro	0.2	75%	0.3	64%	0.3	57%
	North	0.3	75%	0.7	65%	0.9	56%
	Loma	0.2	75%	0.5	64%	0.6	56%
	Kobe	0.3	73%	0.6	64%	0.7	57%

5. Conclusion

Seismic-induced pounding is a serious incident that dramatically changes the seismic responses and affects the dynamic characteristics of adjacent buildings. Furthermore, the dynamic characteristics of buildings, such as vibration modes and frequencies, are modified by the stress and strain characteristics of the soil under the foundations of the buildings; in some cases, dominate the seismic performance.

In this research, seismic response of specific case of four symmetric adjacent High-Rise Buildings (HRBs) in group with two-side projection raft foundation of each building was studied under four different earthquakes considering the SSI effect. Mutual pounding effect between the adjacent 4HRBs was studied in presence of irregular distribution of stresses in the soil beneath the raft foundations owing to the two-side foundation projection.

To find the most appropriate way to mitigate the effect of collision between the adjacent 4HRBs, three approaches were proposed taking into consideration the SSI effect. The first approach is improving the soil bearing capacity under the raft foundation of the four adjacent buildings using driven piles under half of each raft foundation in the highly stressed zone. The second method is connecting the adjacent 4HRBs using Fluid Viscous Links (FVLs). And the third method is merging the two previous methods. The seismic responses of the adjacent 4HRBs (in terms of lateral displacements, base shear forces, and base moments) were compared with the responses of a similar single HRB with two-side projection foundation as a reference case. The ratios between the corresponding values of the measured responses, see Table 18, are used for the comparison to understand the deviation of the responses of pounding HRBs from the responses of a single HRB under different earthquakes considering SSI. Additionally, the efficiency of the proposed pounding mitigation procedures is investigated by comparing the responses of the adjacent HRBs when applying mitigation procedure to the responses of the adjacent HRBs without mitigation procedures. The following conclusions could be drawn:

- Although there is a reduction in the lateral displacement of the adjacent HRBs without mitigation procedure (GC1) compared with the corresponding values of the single HRB (SC) for some earthquakes, there is an enormous increase in the base shear and the base moment values reaches up to 1.9 times the values of the single HRB case (SC), see Table 18. This is due to the partial confinement in movement of the adjacent buildings and the mutual collision forces between the adjacent buildings.
- Improving the soil bearing capacity resulted in reducing the lateral displacements of the adjacent HRBs (GC2) compared with the single HRB (SC) for all earthquakes. Besides, the max increase in base shear and base moment values are 1.5 and 1.4 times the values of the single HRB (SC), respectively, see Table 18. Furthermore, the reduction in the maximum base shears of case (GC2) relative to case (GC1) is (22-23%), and the reduction in the maximum base moments of case (GC2) relative to case (GC1) is (25-26%) under the considered earthquakes, as seen in Table 18. In another word, soil improvement procedure reduces the lateral displacements, base shears, and base moments of pounding HRBs compared to the case without improvement. These results imply the effectiveness of the soil improvement with driven piles as a procedure that mitigates the effect of pounding.
- Connecting the adjacent 4HRBs with fluid viscous links, case (GC3), resulted in reduction in the lateral displacements of case (GC3) relative to case (GC1) ranges from 68% to 71%. Moreover, the reduction in base shear of case (GC3) relative to case (GC1) is 45%, and the reduction in base moment of case (GC3) relative to case (GC1) ranges from 38% to 39%. Thus, connecting adjacent HRBs with fluid viscous links in presence of the combined effects of the collision and the soil stress irregularity not only reduces lateral displacements, but also enormously mitigates the other seismic responses of such buildings as base shears and base moments.

- Merging between the procedures of improving the soil bearing capacity and connecting the high-rise buildings with FVLs caused a remarkable mitigation in the seismic responses of the adjacent HRBs under the combined effects of collision and soil stress irregularity. Results showed that the reduction in maximum lateral displacements of case (GC4) relative to case (GC1) ranges from 73% to 75%, while the reduction in maximum lateral displacements of case (GC3) relative to case (GC1) ranges from 68% to 71%. Thus, improving soil bearing capacity along with connecting buildings with FVLs has an advantage over using FVLs only in reducing lateral displacements of adjacent buildings exposed to seismic-induced pounding. Additionally, the values of the reduction in the maximum base shear of case (GC4) relative to case (GC1) range from 64% to 65%, and the values of the reduction in the maximum base moment of case (GC4) relative to case (GC1) range from 56% to 57%, as in Table 18. The procedure of improving soil bearing capacity under raft foundations of adjacent HRBs alongside with connecting the HRBs using fluid viscous links showed promising results in mitigating the effects of seismic-induced-collision on the response of adjacent buildings impose irregular soil stress.

References

[1] Jankowski, R. and Mahmoud, S., (2016), "Linking of adjacent three-storey buildings for mitigation of structural pounding during earthquakes", Bull Earthquake Eng., **14**, 3075-3097. https://doi.org/10.1007/s10518-016-9946-z

[2] Barros R. C. and Khatami S. M., (2013), "Damping ratios for pounding of adjacent buildings and their consequence on the evaluation of impact forces by numerical and experimental models", Mecânica Experimental, 22, 119-131.

[3] Licari M.,Sorace S. and Terenzi G., (2015), "Nonlinear modeling and mitigation of seismic pounding between R/C frame buildings", Journal of Earthquake Engineering, **19(**3), 431-460. https://doi.org/10.1080/13632469.2014.984370

[4] Polycarpou P. C. and Komodromos P., (2011), "Numerical investigation of potential mitigation measures for poundings of seismically isolated buildings", Earthquakes and Structures, **2(**1), 1-24. https://doi.org/10.12989/eas.2011.2.1.001.

[5] Lin W., Wang Q., Li J., Chen S., and Qi A., (2017), "Shaking table test of pounding tuned mass damper (PTMD) on a frame structure under earthquake excitation", Computers and Concrete, **20**(5), 545-553. https://doi.org/10.12989/cac.2017.20.5.545

[6] Skrekas P., Sextos A. and Giaralis A., (2014), "Influence of bi-directional seismic pounding on the inelastic demand distribution of three adjacent multi-storey R/C buildings", Earthquakes and Structures, 6**(**1), 71-87. https://doi.org/10.12989/eas.2014.6.1.071

[7] Khatiwada S., Larkin T., and Chouw N., (2014), "Influence of mass and contact surface on pounding response of RC structures", Earthquakes and Structures, **7**(3), 385-400. https://doi.org/10.12989/eas.2014.7.3.385

[8] Polycarpou P. C., Papaloizou L., KomodromosP. and Charmpis D. C., (2015), "Effect of the seismic excitation angle on the dynamic response of adjacent buildings during pounding", Earthquakes and Structures, **8**(5), 1127-1146. https://doi.org/10.12989/eas.2015.8.5.1127

[9] Lin W., Lin Y., Song G., and Li J., (2016), "Multiple Pounding Tuned Mass Damper (MPTMD) control on benchmark tower subjected to earthquake excitations", Earthquakes and Structures, **11**(6), 1123-1141. https://doi.org/10.12989/eas.2016.11.6.1123

[10] Amiri G. G., Shakouri A., Veismoradi S. and Namiranian P., (2017), "Effect of seismic pounding on buildings isolated by triple friction pendulum bearing", Earthquakes and Structures, 12(1), 35-45. https://doi.org/10.12989/eas.2017.12.1.035.

[11] Bi K., Hao H., and Sun Z., (2017), "3D FEM analysis of earthquake induced pounding responses between asymmetric buildings", Earthquakes and Structures, **13**(4), 377-386. https://doi.org/10.12989/eas.2018.13.4.377

[12] Kheyroddin A., Kioumarsi M., Kioumarsi B. and Faraei A., (2018), "Effect of lateral structural systems of adjacent buildings on pounding force", Earthquakes and Structures, **14**(3), 229-239. https://doi.org/10.12989/eas.2018.14.3.229.

[13] Jiang S., Zhai C., Zhang C., and Ning N., (2018), "Analysis of seismic mid-column pounding between low rise buildings with unequal heights", Earthquakes and Structures, **15**(4), 395-402. https://doi.org/10.12989/eas.2018.15.4.395

[14] Karabork T. and Aydin E., (2019), "Optimum design of viscous dampers to prevent pounding of adjacent structures", Earthquakes and Structures, **16**(4), 437-453. https://doi.org/10.12989/eas.2019.16.4.437

[15] Abdel Raheem S. E., Fooly M. Y.M., Omar M. and Abdel Zaher A. K., (2019), "Seismic pounding effects on the adjacent symmetric buildings with eccentric alignment", Earthquakes and Structures, **16**(6), 715-726. https://doi.org/10.12989/eas.2019.16.6.715.

[16] Shi J., Bamer F., and Markert B., (2019), "A substructure formulation for the earthquake-induced nonlinear structural pounding problem", Earthquakes and Structures, **17**(1), 101-113. https://doi.org/10.12989/eas.2019.17.1.101.

[17] Abdel Raheem S. E., Fooly M.Y.M., Abdel Shafy A.G.A., Abbas Y. A., Omar M., Abdel Latif M.M.S. and Mahmoud S., (2018), "Seismic pounding effects on adjacent buildings in series with different alignment configurations", Steel and Composite Structures, 28(3), 289-308. https://doi.org/10.12989/scs.2018.28.3.289.

[18] Naserkhaki S., El-Rich M., Abdul Aziz F.N.A. and Pourmohammad H., (2014), "Pounding between adjacent buildings of varying height coupled through soil", Structural Engineering and Mechanics, **52**(3), 573-593. https://doi.org/10.12989/sem.2014.52.3.573.

[19] Rahimi S. and Soltanim M., (2017), "Expected extreme value of pounding force between two adjacent buildings", Structural Engineering and Mechanics, **61**(2), 183-192. https://doi.org/10.12989/sem.2017.61.2.18.

[20] Shehata E. A., M. A. Tarek, G. A. Aly, M. M. Ahmed, and A. S. Yasser, (2021), "Seismic pounding between adjacent buildings considering soil-structure interaction", Earthquakes and Structures, **20**(1), 55-70. https://doi.org/10.12989/eas.2021.20.1.055.

[21] F. Kazemi, M. Miari, and R. Jankowski, (2020), "Investigating the effects of structural pounding on the seismic performance of adjacent RC and steel MRFs", Bulletin of Earthquake Engineering, **19**, pages317–343. https://doi.org/10.1007/s10518-020-00985-y

[22] Farghaly A. A., (2017), "Seismic analysis of adjacent buildings subjected to double pounding considering soil–structure interaction", Int J Adv Struct Eng, **9**, 51–62. https://doi.org/10.1007/s40091-017-0148-y.

[23] Far H., (2017), "Advanced computation methods for soil-structure interaction analysis of structures resting on soft soils.", Int J Geotech Eng, 1–8.

[24] Stewart JP, Fenves GL, Seed RB., (1999), "Seismic soil-structure interaction in buildings. I: analytical methods.," J Geotech Geoenviron Eng, 125:26–37.

[25] M. Miari, K. K. Choong, and R. Jankowski, (2019), "Seismic pounding between adjacent buildings: Identification of parameters, soil interaction issues and mitigation measures", Soil Dynamics and Earthquake Engineering, vol. 121, pp. 135-150.

[26] M. Miari, K. K. Choong, and R. Jankowski, (2021), "Seismic pounding between bridge segments: a state-of-the-art review," Archives of Computational Methods in Engineering, vol. 28, no. 2, pp. 495-504.

[27] Mahmoud S, Abd-Elhamed A, Jankowski R., (2013), "Earthquake-induced pounding between equal height multi-storey buildings considering soil-structure interaction.", Bull Earthq Eng, 11:1021–48.
[28] Naserkhaki S, Aziz FNA, Pourmohammad H., (2012), "Earthquake induced pounding between adjacent buildings considering soil-structure interaction.", Earthq Eng Earth Vib, 11:343–58.
[29] Madani B, Behnamfar F, Riahi HT., (2015), "Dynamic response of structures subjected to pounding and structure–soil–structure interaction.", Soil Dyn Earthq Eng, 78:46–60.
[30] M. Miari and R. Jankowski, (2022), "Analysis of pounding between adjacent buildings founded on different soil types", Soil Dynamics and Earthquake Engineering, vol. 154, p. 107156.
[31] M. Miari and R. Jankowski, (2021), "Pounding between high-rise buildings founded on different soil types", 17th World Conference on Earthquake Engineering, Sendai, Japan.
[32] Mahmoud S, Gutub SA., (2013), "Earthquake induced pounding-involved response of base isolated buildings incorporating soil flexibility.", Adv Struct Eng, ;16:2043–62.
[33] ECP-203 (2007), "Egyptian code for design and construction of reinforced concrete structures", (HBRC), Ministry of Housing, Utilities and Urban Planning, Cairo.
[34] ECP-201(2008), "Egyptian code for calculating loads and forces in structural work and masonry", (HBRC), Ministry of Housing, Utilities and Urban Planning, Cairo.
[35] COSMOS. COSMOS Virtual Data Center, <http://db.cosmos-eq.org/>; 2011.
[36] Nathan M. Newmark and Emilio Rosenblueth, (1971), "Fundamentals of Earthquake Engineering", Prentice-Hall, Englewood Cliffs, N.J.
[37] Aidcer L. Vidot, Luis E. Suarez, Enrique E. Matheu, and Michael K. Sharp, (2004), "Seismic Analysis of Intake Towers Considering Multiple-Support Excitation andSoil-Structure Interaction Effects", Geoteclinical and Structures Laboratory, U.S. Army Engineer Research and Development Center, 3909 Halls Ferry Road, Vicksburg, MS 39180-6199.
[38] Anagnostopoulos SA., (1988), "Pounding of buildings in series during earthquakes.", Earthq Eng Struct Dyn, 16(3), 443–456.
https ://doi.org/10.1002/eqe.42901 60311
[39] Anagnostopoulos SA., (2004), "Equivalent viscous damping for modelling inelastic impacts in earthquake pounding problems", Earthquake Engineering and Structural Dynamics, **33**(8), 897–902.
https://doi.org/10.1002/eqe.377
[40] Jankowski R (2005), "Non-linear viscoelastic modelling of earthquake induced structural pounding." Earthq Eng Struct Dyn, **34**, 595–611.

Statements & Declarations

- **Funding**

The authors did not receive any support from any organization for the submitted work, and they have no relevant financial or non-financial interests to disclose

- **Competing Interests**

The authors have no competing interests to declare that are relevant to the content of this article and have no affiliations with any organization or entity with any financial interest or non-financial interest in the subject matter discussed in this manuscript

- **Author Contributions**

All authors contributed to the study conception and design, data collection, data interpretation, work draft, and read and approved the manuscript.

التأثير المشترك للتصادم الناجم عن الزلازل وعدم انتظام إجهاد التربة على الاستجابة الزلزالية للمباني الشاهقة المتجاورة: التقييم والتخفيف

الملخص

يمثل التوزيع غير المنتظم للاجهادات على التربة تحت أساسات المباني المتجاورة تحديًا كبيرًا في الهندسة الإنشائية، خاصة في المباني المعرضة للزلازل. من المشكلات الخطيرة الأخرى التي تواجه المباني المتجاورة المعرضة للزلازل هي الاصطدام الذي يؤثر بشدة على سلوك المباني ويغير توزيع ضغوط التربة تحت أساسات المباني. يبحث هذا البحث في الاستجابات الزلزالية للمباني الشاهقة المتجاورة التي تسبب توزيع غير منتظم لضغط التربة والمعرضة للاصطدام الناجم عن الزلازل مع الأخذ في الاعتبار التأثير المتبادل بين المبنى والتربة. لهذا الغرض، تم إجراء تحليل ديناميكي رقمي غير خطي للنماذج ثلاثية الأبعاد لأربعة من المباني الشاهقة المتجاورة لدراسة تأثير التصادم الناجم عن الزلازل وعدم انتظام إجهاد التربة على الاستجابة الزلزالية للمباني الشاهقة المتجاورة. تم اقتراح ثلاثة نهج للتخفيف من تأثير التصادم الناجم عن الزلازل وعدم انتظام إجهاد التربة على الاستجابة الزلزالية للمباني وهي، تحسين قدرة تحمل التربة في المنطقة عالية الاجهاد، ربط المباني المتجاورة عن طريق روابط الموائع اللزجة (Fluid Viscous Links)، والجمع بين النهجين السابقين. تمت دراسة النماذج ثلاثية الأبعاد لمجموعة المباني الشاهقة المتجاورة تحت تاثير زلازل مختلفة لفحص الطرق الثلاثة المذكورة أعلاه. يظهر النهج المشتمل على دمج كل من تحسين قدرة تحمل التربة وربط المباني المتجاورة عن طريق روابط الموائع اللزجة نتائج واعدة في تخفيف آثار الاصطدام؛ حيث يخفف بشكل كبير من آثار الاصطدام بين المباني المتجاورة من حيث الحد من الإجهادات والازاحات بالمباني وكذلك التحكم في الإجهاد غير المنتظم في التربة تحت أساسات مثل هذه المباني.